Abstract

A computational investigation has been adopted for design an optical system for infrared (IR) homing head, operated in region of spectrum (3-5) μm. The characteristics of the present optical system design include the modulation transfer function (MTF) and spot size. These characteristics are determined which give the efficiency and accuracy of the design optical system. Our work has been performed in two stages namely; design and improvement, to get the efficiency of the developed optical system.

The design stage depends originally on a standard optical system for IR homing head. Some modifications and improvements have been imposed on the standard design to achieve a new one of high quality characteristics.

These improvements include choosing the most suitable materials and features for each optical element in the developed design.

An improvement stage was then followed on the radius of curvature of correcting lens, which has process carried out by Zemax software to determine the most favorable optical properties i.e. spherical aberration, size of spot, and size and shape of the system.

It is appears from all results that the best suggested suitable materials for IR homing head is Sapphire when use in manufacture dome and correcting lens. Also, the Germanium materials can not be used in manufacture the dome.

Acknowledgement

I would like to express my sincere thanks and deep gratitude to the late **Prof. Dr. Sabah M. Juma, Dr. Fatin A. Al-Moudarris** and **Dr. Ayad A. Al-Ani** for supervising this work and for their support and encouragement throughout the research.

Also, I would like to thank **Mrs. Suha Mousa, Mr. Mohammed Saheb,** and **Mr. Abrahem A. Sadiq** for their valuable assistance during the work.

I am grateful to the Dean of College of Science and the staff of the Department of Physics at Al-Nahrain University for their valuable support and cooperation.

Last but not least, I would like to record my deep affection and thanks to **my family** for their moral support and patience throughout this work.

Haala

APPENDIX

Optical Materials Selection Guide

Barium Fluoride (BaF_2)

Barium Fluoride can be used in the ultraviolet, visible and infrared spectral regions. Barium fluoride has transmission above 90% between 0.25 and 9.5µm.

Barium Fluoride is half as hard as Calcium Fluoride and also more susceptible to thermal shock. However, it is commonly used in cryogenically cooled thermal imaging systems. It is somewhat more expensive than Calcium Fluoride and not as readily available in large sizes.

Property	**Specification**
Transmission Range	0.15 to 12.5µm
Density	4.89 g/cm³
Thermal Expansion Coefficient	18.1x10-6 /°C@20°C+/-100°C
Surface Finish	Polishes of 20-10 scratch-dig are mostly specified for use in UV and visible applications. Typical specifications for surface quality in the infrared are a 40-20 scratch dig in the 0.75 to 3µm spectral region and 60-40 scratch-dig for the 3-7µm area. BaF_2 is diamond turnable.
Surface Figure	Surface figure of a 1/10 wave to 1/2 wave @0.6328 µm are specified mostly on lenses for ultraviolet and visible use. In the infrared, typical required surface figure ranges from 1/2 wave to 2 waves @0.6328 µm depending on the system performance requirements.
AR Coating Options	Typical available coatings for BaF_2 include BBAR for 0.8 to 2.5 µm, 3 to 5µm or the 1 to 5µm spectral regions.
Typical Applications	Cryogenically cooled thermal imaging, Astronomical, Laser applications.
Products Manufactured	Lenses, Aspheric lenses, Windows, Optical Beamsplitters, Optical Filters, Wedges, Prisms.

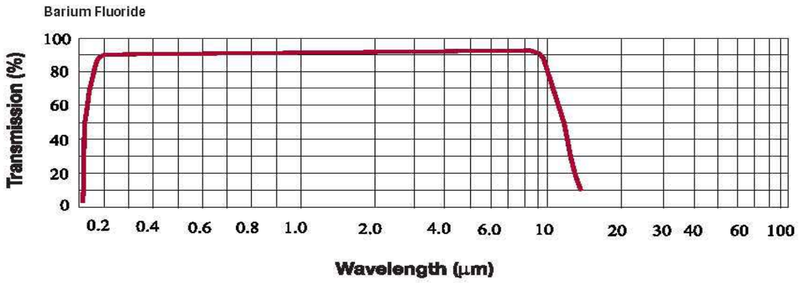

Wavelength µm	**Index of Refraction (n)**
1.700	1.466
2.152	1.464
3.422	1.459
4.000	1.455
6.238	1.442
7.268	1.433
10.346	1.396

Germanium (Ge)

Germanium has the highest index of refraction of any commonly used infrared transmitting materials. It is a very popular material for systems operating in the 3-5 or 8-12µm spectral regions. Germanium blocks UV and visible light and in the infrared up to about 2µm. Its high index is desirable for the design of lenses that might not otherwise be possible. Germanium has nearly the highest density of the infrared transmitting materials and this should be taken into consideration when designing for weight restricted systems. Germanium is subject to thermal runaway, meaning that the hotter it gets, the more the absorption increases. Pronounced transmission degradation starts at about 100°C and begins rapidly degrading between 200°C and 300°C, resulting in possible catastrophic failure of the optic.

Property	**Specification**
Transmission Range	2 to 14µm
Density	5.33g/cm^3
Thermal Expansion Coefficient	2.3x10-6 /°K @ 100°K, 5.0x10-6 /°K @ 200°K, 6.0x10-6 /°K @ 300°K
Surface Finish	Typical specifications for surface quality in the infrared are 40-20 or 60-40 scratch dig in the 2 to 7µm spectral region and 60-40, 80-50 or 120-80 scratch- dig for the 7-14µm area, depending upon system performance requirements. Diamond turned surface finishes of 120 Angstroms rms or better are typical.
Surface Figure	Surface figure: In the infrared, typical surface figure ranges from 1/2 wave to 2 waves @0.6328µm depending on the system performance requirements.
AR Coating Options	Typical available coatings for Germanium include BBAR for 3 to 5µm, 8 to 12µm, and the 3 to 12µm spectral regions. Many application specialized bands are possible between the 2 and 14µm.
Typical Applications	Thermal imaging, FLIR.
Products Manufactured	Lenses, Aspheric Lenses, Binary (Diffractive) Lenses, Windows, Optical Beamsplitters, Optical Filters, Wedges.

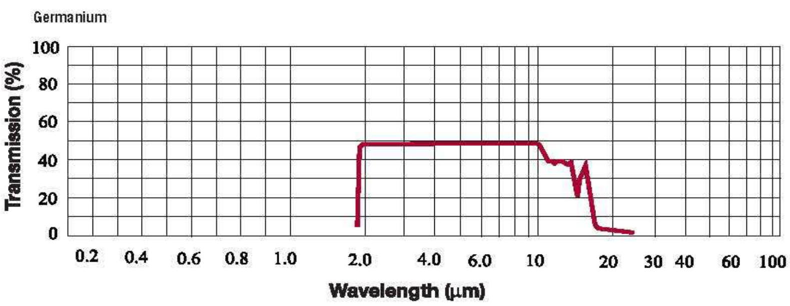

Wavelength µm	**Index of Refraction (n)**
2.5	4.046
3.0	4.044
4.0	4.025
8.0	4.007
10.0	4.005
12.0	4.004
14.0	4.003

Magnesium Fluoride (MgF_2)

Magnesium Fluoride is used for optical elements in both the infrared and ultraviolet. Its useful transmission range is from .19µm; to 6.5µm. The refractive index varies from about 1.48 to 1.3. Magnesium Fluoride is a birefringent material and this aspect should be taken into consideration before selection of this material in an optical design. Janos uses only VUV grade material, with the C-axis oriented to minimize birefringence. Irradiation does not lead to color centers. This VUV material is the least susceptible to radiation induced color centers.

Magnesium Fluoride is one of the lowest index infrared materials, second only to Lithium Fluoride. It is resistant to thermal and mechanical shock. The material is twice as hard as Calcium Fluoride but only half as hard as Germanium. Magnesium Fluoride is significantly more expensive than Calcium Fluoride and Barium Fluoride, but usually not more expensive than Lithium Fluoride. Magnesium Fluoride is similar to Calcium Fluoride in its resistance to water.

Property	**Specification**
Transmission Range	0.121µm to 7.0µm
Density	3.177g/cm^3
Thermal Expansion Coefficient	13.7x10-6 /°C Parallel to C-axis 8.48 x10-6 /°C Perpendicular to C-axis
Surface Finish	Polishes of 10-5, or 20-10 scratch-dig are achieved at extra costs respectively mainly for UV applications. Typical specifications for surface quality in the visible and near infrared regions are a 40-20 and 60-40 scratch dig in the 3 to 7µm range. MgF_2 is diamond turnable.
Surface Figure	In the UV and Visible spectral regions, surface figure ranges from 1/10 wave to 1/2 wave @0.6328µm. In the infrared, typical required surface figure ranges from 1/2 wave to 2 waves @0.6328µm and are specified depending on the system performance requirements.
AR Coating Options	Magnesium Fluoride can be AR coated for use in the infrared but generally without much improvement in transmission due to its low index of refraction and already high transmission.
Typical Applications	Thermal imaging, Astronomical, Excimer laser applications.
Products Manufactured	Lenses, Aspheric lenses, Windows, Optical Beamsplitters, Optical Filters, Wedges, Prisms.

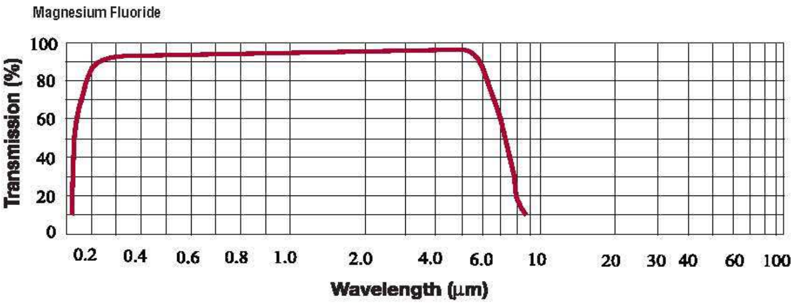

Wavelength µm	**Index of Refraction (n)**
0.114	1.7805
0.118	1.6800
0.130	1.5560
0.150	1.4800
0.170	1.4470
0.190	1.4310
0.300	1.4000
0.700	1.3760

Calcium Fluoride (CaF_2)

Calcium Fluoride can be used in the ultraviolet, visible and infrared spectral regions. Calcium Fluoride has a transmission above 90% between 0.25 and 7μm.

Calcium Fluoride is twice as hard as Barium Fluoride and also less susceptible to thermal shock. However, it is commonly used in cryogenically cooled thermal imaging systems. It is less expensive than Barium Fluoride. CaF_2 is diamond turnable

Property	**Specification**
Transmission Range	0.13μm to 7.0μm
Density	3.18 g/cm^3
Thermal Expansion Coefficient	18.85x10-6 / °C
Surface Finish	Polishes of 20-10 scratch-dig are mostly specified for use in UV and visible applications. Typical specifications for surface quality in the infrared are a 40-20 scratch dig in the 0.75 to 3μm spectral region and 60-40 scratch-dig for the 3-7μm area.
Surface Figure	Surface figure: In the UV and Visible spectral regions, surface figure ranges from 1/10 wave to 1/4 wave @ 0.6328μm. In the infrared, typical required surface figure ranges from 1/4 wave to 2 waves @ 0.6328 μm and are specified depending on the system performance requirements.
AR Coating Options	Available coatings for CaF_2 include BBAR for 0.8 to 2.5μm, 3 to 5μm or the 1 to 5μm spectral regions
Typical Applications	Cryogenically cooled thermal imaging, Astronomical, Microlithography, Excimer Laser applications.
Products Manufactured	Lenses, Aspheric lenses, windows, Optical Beamsplitters, Optical Filters, Wedges, Prisms.

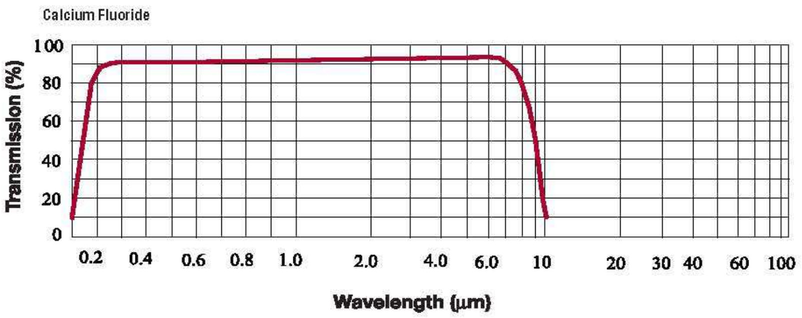

Wavelength μm	**Index of Refraction (n)**
1.0600	1.428
2.0582	1.424
4.0000	1.410
5.8932	1.387
8.2505	1.344
9.4291	1.316

Lithium Fluoride (LiF)

Lithium Fluoride has the lowest index of refraction of all the common infrared materials. LiF is slightly plastic, and has a relatively high thermal expansion coefficient. It is also the most expensive of the Fluoride series of crystals.

Property	**Specification**
Transmission Range	0.121μm to 5.0μm
Density	2.639 g/cm^3
Thermal Expansion Coefficient	37x10-6 / °C
Surface Finish	Typical specifications for surface quality in the infrared are a 40-20 scratch dig in the 0.75 to μm spectral region and 60-40 or 80-50 scratch-dig for the 3-7μm area depending upon system performance requirements. LiF is diamond turnable.
Surface Figure	In the infrared, typical surface figure ranges from 1/2 wave to 4 waves @0.6328μm depending upon system performance requirements.
AR Coating Options	LiF can be AR coated for use in the infrared, but generally without much improvement in transmission due to its low index of refraction and already high transmission
Typical Applications	Thermal imaging, Astronomical, Excimer laser applications.
Products Manufactured	Lenses, Aspheric lenses, Windows, Wedges, Prisms.

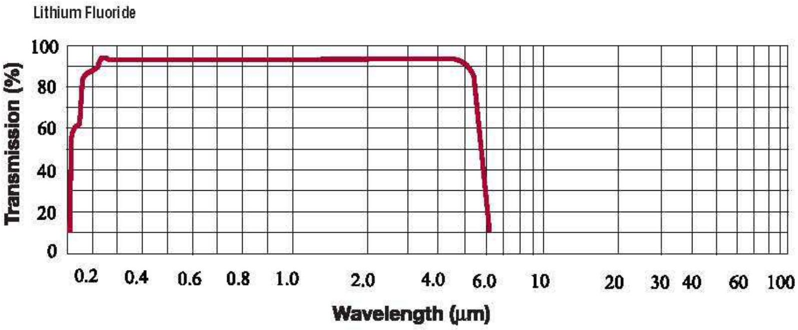

Wavelength μm	**Index of Refraction (n)**
1.0	1.387
2.0	1.379
3.0	1.367
4.0	1.349
5.0	1.327
5.8	1.304

Certification

We certify that this thesis entitled **"A Computational Investigation on the Effect of Lens Material on the Aberrations of an Infrared Optical System"** was prepared by **Miss. Haala Fadhil Al-Baldawi,** under our supervision at the College of Science of Al-Nahrain University in partial fulfillment of the requirements for the degree of **Master of Science** in physics.

Signature:
Name: **Prof. Dr. Sabah M. Juma**
(Supervisor)
Data:

Signature:
Name: **Dr. Fatin Almoudarris**
(Supervisor)
Data:

Signature:
Name: **Assist Prof. Dr. Ayad A. Al-Ani**
(Supervisor)
Data:

Signature:
Name: **Dr. A. K. Ahamed**
(Head of Department)
Data:

CHAPTER FIVE

CONCLUSIONS AND SUGGESTION FOR FUTURE WORK

٥,١ Conclusions

From our results we can conclude that:

(a) The efficiency of the adopted system is dependent on the radius of curvature for correcting lens.

(b) In general, the best suggested suitable materials for IR homing head are Sapphire and Germanium when used in correcting lens. Another materials gives a high distortion in image.

(c) The best optical system was obtained when the dome and correcting lens are made of Sapphire material.

(d) The Germanium material can not be used in manufacture dome because its distort the size and the shape of system.

5.2 Suggestions for future work

From the results of the present work, one may recommend the following projects for future work.

(a) An improvement process for materials in order to select another infrared material with regard to paraxial lens parameters and image quality evaluation.

(b) The optical transfer function and statistical optics important tools to improve the performance of any optical element or system, so they should be considered as an advance research.

(c) Studying the effects for field of view and temperature for optical system.

(d) Studying the off-axis rays for optical system.

CONTENTS

CURRICULUM VITAE

الاسم: هالة فاضل عباس البلداوي

عنوان السكن : حي الكرادة ، محلة ٩٠١ ، زقاق ١٥ ، دار ٦

الايميل: halafadal@yahoo.com

الهاتف : لا يوجد

تاريخ المناقشة : ١١ \ ١ \ ٢٠٠٧

اسم المشرف : د. اياد عبد العزيز العاني

اسم الرسالة: دراسة حاسوبية عن تأثير مادة العدسة على زيوغ منظومة تحت الحمراء بصرية

A COMPUTATIONAL INVESTIGATION ON THE EFFECT OF LENS MATERIAL ON THE ABERRATIONS OF AN INFRARED OPTICAL SYSTEM

Examination Committee Certification

We certify that we have read the thesis entitled **"A Computational Investigation on The Effect of Lens Material on The Aberrations of an Infrared Optical System "** and as an examination committee, examined the student **Miss Haala Fadhil A. Al-Baldawi** on its contents, and that in our opinion it is adequate for the partial fulfillment of the requirements of the degree of **Master of Science in Physics**.

Signature:
Name: **Dr. Ahmad K. Ahmad**
Title: **Assistant Professor**
Chairman
Data:

Signature:
Name: **Dr. Ali H. Al-Hamdani**
Title: **Assistant Professor**
Member
Data:

Signature:
Name: **Mohammed A. Saleh**
Title: **Senior Scientific Researcher**
Member
Data:

Signature:
Name: **Dr. Ayad A. Al-Ani**
Title: **Assistant Professor**
Supervisor
Data:

Approved by the University Committee of Postgraduate Studies

Signature:
Name: **Dr. Laith A. Al-Ani**
Title: **Assistant Professor**
Dean of the College of Science
Data:

CHAPTER ONE
INTRODUCTION

1.1 Infrared Systems

In everyday life all the people in the world encounter many different types of radiation. Seemingly different forms, such as sunlight, heat, radio waves, and x- rays to name only a few, are inherently similar in nature that can be conveniently grouped under a single classification, called electromagnetic radiation. It is common practice to describe these radiations by their position in the electromagnetic spectrum; it is an arrangement of the various radiations by wavelength or frequency. All of the radiations obey similar laws of reflection, refraction, diffraction, and polarization. The velocity of propagation in vacuum, popularly called the velocity of light is the same for all. They differ from one another only in wavelength and frequency. The infrared (IR) radiation means that portion of the electromagnetic spectrum that lies between visible light on the one hand and microwaves on the other. Expressed quantitatively, it is the region that extends from a wavelength of (0.75 to 1000) μm, which as a portion of the electromagnetic spectrum that can be shown in figure 1.1 **[Hudson 1969]**.

The term “target” refers collectively to those objects that IR systems are designed to detect. Although specific details on the military application of IR technique and the radiating characteristics of some targets are classified by the military, reasonably accurate estimates can often be made by applying the radiation laws and certain other information readily available in the open literature. However, as far as the present work is concerned, it should be mentioned that clear and detailed accounts of many purpose-built IR systems for military applications are still classified or to be little found in the published literature.

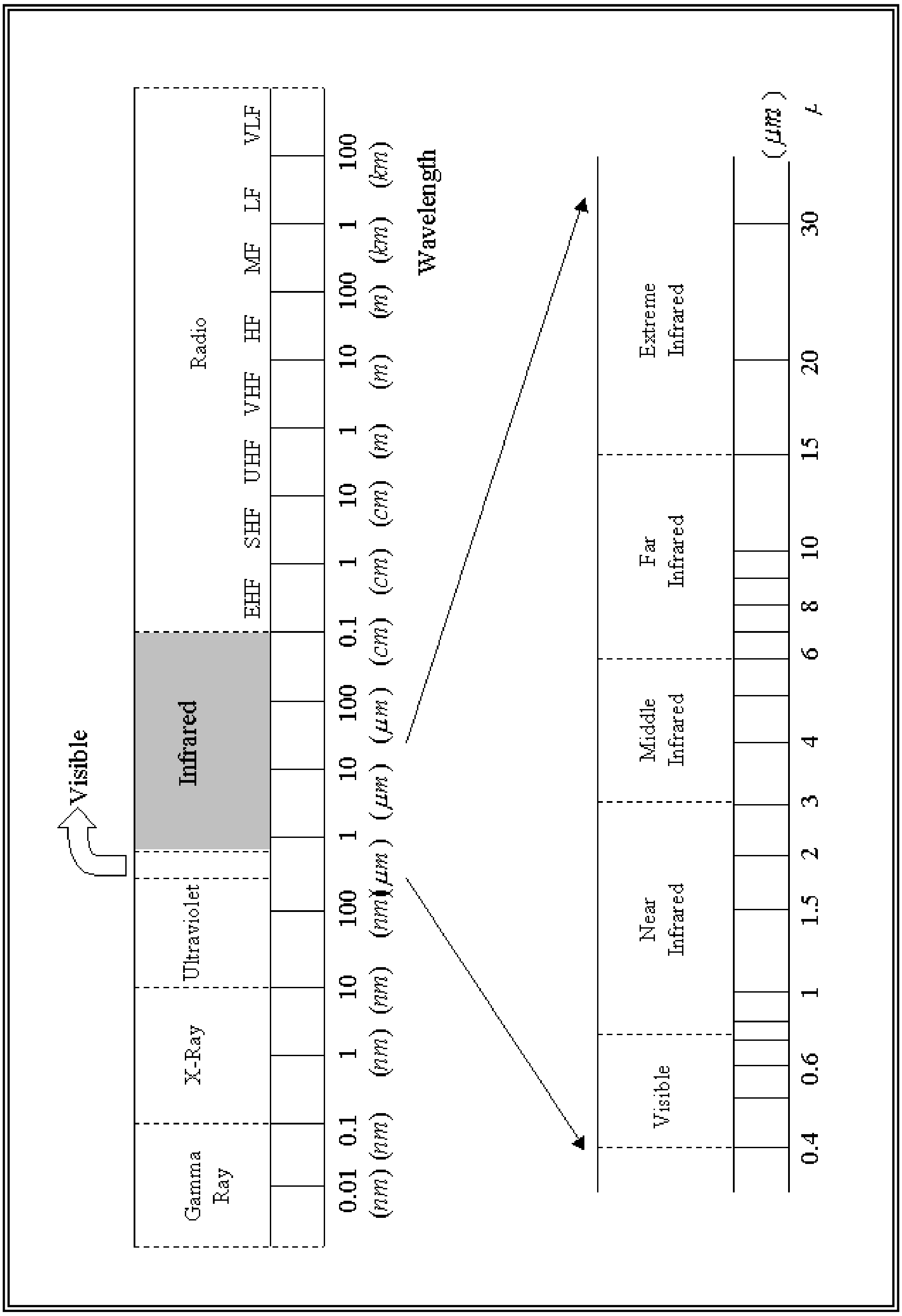

Figure 1.1 Electromagnetic spectrum **[Hudson 1969]**

1.2 Design of Optical System

The optical design process should be consistent with the required applications. Many applications require some specialized design and a successful optical system design requires from the designer careful consideration of the design specifications, which is the most important step in the optical design process. The ordinary design process can be broken down into the following three steps **[Shannon 1997]**:

(a) Choosing the type of the design to be executed, that is, the number and types of elements and their general configuration.

(b) Determination of the powers, materials, thickness, and spacing of the elements. Which are usually selected to control the chromatic aberrations and radius of curvature of the system, as well as the focal length, working distance, field of view, and aperture diameter.

(c) Adjusting the shapes of the various elements or components to correct the aberrations to the desired and optically acceptable values.

The optics used in an IR homing head shows the configuration of the optical system that consists of dome, primary mirror, secondary mirror, and correcting lens **[Dubner 1959]**. Once the optical system has been specified and built the next task is to test its performance. The usual optical tests are measuring the modulation transfer function “MTF”, transmission, and optical spot size.

1.3 Optical Design Parameters

The optical design parameters known as “lens parameters or degrees of freedom ”, enable the designer to achieve an optimum design for the desired application by making changes i.e. modifications to these parameters to minimize the cost and size while maintaining the design required properties. These parameters are **[Kingslake 1978]**:

- The radii of curvature of the surfaces
- Surface shape
- Thickness
- Air spaces
- Refractive indices
- Dispersive power of the glass used for separated lens elements
- Position of the “stop” or aperture – limiting diaphragm or lens mount.

1.4 Historical Review

The application of IR techniques has been known since the beginning of the twentieth century. As early as 1910, many workers were intrigued by the possibility of heat seekers and were proposing a wide variety of IR search devices. In the 1920's the availability of the thallous sulfide detector encouraged a new generation of workers to reinvent IR search device. When the lead sulfide detector appeared in mid-1950's photon detectors sensitive in the (3 to 5)μm window were developed. Further developments were introduced in the early 1960's when small and reliable cooling devices became available for these (3 to 5)μm detectors **[Hudson 1969]**.

Infrared technology was born during the period between World Wars I and II, is marked by the development of photon detectors and image converters. Between the period 1940-1945 many research programs have been developed to produce thermal cameras **[Hudson 1969]**.

In 1952, the U.S Army built the first scanning thermal imager, which were called thermographs **[Lioyd 1975]**.

Dubner [1959] has shown that the optics used in IR missile-seeker results from a series of design compromises involving sensitivity, resolution, and geometry. Since the optical parts of the system must be contained in a prescribed enclosure, the geometry problem was the most dominant. The optical system consisted of a dome, primary mirror, secondary mirror, correcting lens, reticle, and detector.

Scott [1959] has shown that the main differences between the optics of an IR system and visible system result from the image size requirements in the two portions of the spectrum. Any optical system no mater how perfect in design or construction, will be limited in its resolution by diffraction. The effect of this diffraction depend on the sizes of the optics and wavelength of radiation forming the image. In 1960 the next real-time long wavelength device was a ground-based FLIR built by the Perking-Elmer Corporation for the Army. Between 1960 and 1974 at least sixty different Fliers were developed and several hundred were produced **[Lioyd 1975]**.

Rogers [1977] designed two optical systems consisted from four elements of different materials one operated in (8-14)µm and the other operated in (3-5)µm.

Froelich [1980] developed a low-cost IR seeker for man portable terminal homing heads. In order to minimize production costs, the development emphasized on design simplicity and expensive manufacturing processes. Low cost IR seeker engagement parameters represent a short–range round launched over a land combat vehicle. The seeker optical system has an aerodynamically spun dome that holds a roof mirror on the inside cylindrical axis. This provides a rotary field scan.

Baker [1983] described an IR sensor that works in two ways. First: the weapon delivery system can leave the immediate area or take cover when fired, as the missile will not require any further commands from the launcher. Second as the missile home in on radiation produced by virtue of the target physical temperature, it is harder to decoy the missile or camouflage the target to prevent it radiating.

An infrared objective system lens has been designed by **Boutellier [1985]** which provides an infrared lens system for the wavelength range of (3.5-5)µm, that design consists of three lens elements made from silicon, calcium fluoride and silicon, such design intended for use in a thermal imaging device.

The suitability of Zinc Sulfide versus Germanium for the middle negative lens of the Cooke triplet design for the (3-5)µm spectral region is studied by **Sharma [1992]**.

Al-Ani [1995] studied the restoration of atmospherically degraded images. With regard to various kind of optical systems, **Sadiq [2000]** investigated optical systems using the ray tracing analysis to compute wavefront aberrations.

[Habana 2001] design and evaluation of image quality for IR scanner. The Zemax computer program was used by **Zahed [2002]** to design and analyze the homing head systems for tracking targets that emit IR radiation.

In **[2004] Zain Al-Abedeen** studied the atmospheric effects on (3-5)µm band thermal imaging. The Requirements of the optical elements for IR laser range finder were investigated computationally by **Albakir [2005]**.

[Al-kaysi 2006] design and analysis of the four elements objective lens for the 3.2-4.2 µm spectral region.

[Al-Awsi 2006] developed design of optical system for IR homing head and study the homing head characteristic includes PSF, MTF, total spot size and range by implementation of specially developed software for determining these characteristics.

1.5 Aim of the Work

The aim of the work put forward an improved optical design for an IR homing head. The essential parameters that required in an optical system such as spot size and modulation transfer function (MTF) would be investigated and analyzed. The quality of the proposed design would be investigated using various types of optical elements materials in order to improve its performance in Infrared system applications. It has been intended to perform the present investigation computationally by using Zemax software.

The main steps for executing the present research objective is as follows:

(a) Suggesting the IR optical system design based on example found in literature **[Dubner 1959]** and improving this suggested design by choosing different optical materials comport with the design and its application.

(b) Studying the developed system design analytically by determining the effective parameters and their roles.

(c) Obtain some parameters which one can determine the efficiency of the developed design, such as the spot size, and MTF by using Zemax software.

CHAPTER TWO

OPTICAL CONSIDERATION

2.1 Introduction

The principal differences between the optics of infrared systems and visual optical systems result from the image-size requirements in the two portions of the spectrum. Any optical system, no matter how perfect in design or construction, is limited in its resolution by diffraction. The effect of this limitation depends on the size and shape of aperture system and the wavelength of the radiation forming the image. In geometrical optics, the image of a point object is a point. In actual fact an image of a point source produced by an ideal optical system has a central maximum of intensity surrounded by diffraction rings **[Scott 1959]**.

In circular apertures, the diffraction pattern is also circular and the angular separation between the central maximum and the first dark ring is given by **[Donald 1985]**:

$$\text{Sin}\ \theta = \frac{1.22\,\lambda}{D} \tag{2.1}$$

or for small θ , equation. 2.1 rewritten as:

$$\theta \approx \frac{1.22\lambda}{D} \tag{2.2}$$

where θ is measured in radians, λ is the wavelength in meter and D is the diameter of the aperture in meter. Figure (2.1) shows the diffraction of light by circular aperture **[Scott 1959]**. Relation (2.2) may be written as:

$$\frac{d}{\lambda} = 1.22\,F\,\# \tag{2.3}$$

In this form the diameter d of the central maximum is in the same dimensions as the wavelength, while $F\ \#$ is the F-number defined as $F\,\# = \frac{f}{D}$. Here f is the effective focal length of the system.

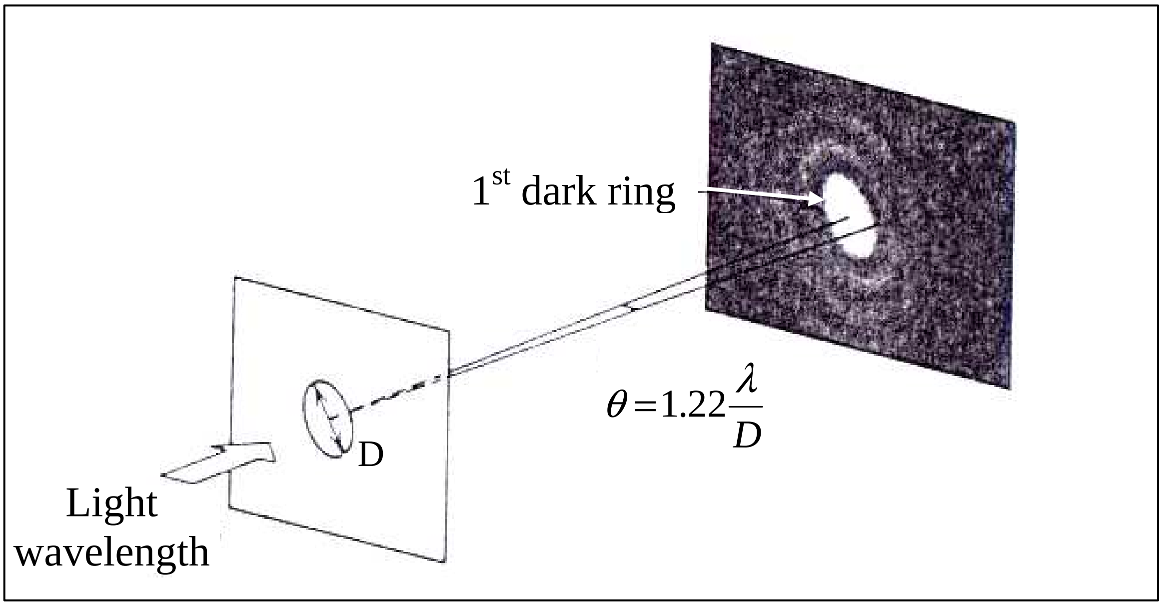

Figure 2.1 Diffraction of light due to Circular aperture **[Donald 1985]**

In designing any optical system, one of the important parameters is the focal length. For the case of spherical mirror, the focal length is given by **[Scott 1959]**:

$$f = \frac{R}{2} \tag{2.4}$$

where R is the radius of curvature of the mirror. The focal length of a lens is given by the following relation **[Scott 1959]**:

$$\frac{1}{f} = (n-1)\left(\frac{1}{R_1} - \frac{1}{R_2} + \frac{(n-1)\,t}{n\,R_1\,R_2}\right) \tag{2.5}$$

where R_1 and R_2 are the radii of curvature of the two spherical surfaces of the lens, t is the thickness of the lens, and n is the refractive index of the lens material. If the effect of thickness " t " of the lens is neglected, equation (2.5) becomes **[Scott 1959]**:

$$\frac{1}{f} = (n-1)\left(\frac{1}{R_1} - \frac{1}{R_2}\right) \tag{2.6}$$

As the rays travel from left to right through a lens, all convex surfaces are taken as having a positive radius and all concave surfaces having a negative radius **[Scott 1959]**.

2.2 Paraxial Optics

Paraxial optics is used to determine the location and the size of image and pupils in the optical system. Sometimes this is referred to as first-order optics or Gaussian optics. The paraxial quantities provide information about ideal image formation in selected set of coordinates. Paraxial variables are angles and ray coordinates that describe the passage of a paraxial ray through the lens. These angles may be selected in object space to correspond to the sine or tangent of the real ray angles that will pass through the lens.

In many of the published literatures, paraxial optics is considered to describe the passage of rays for infintesimal field and aperture. Paraxial optics has considerably greater significance in describing the ideal imaging condition for a lens. It is seen to describe the ray path through the lens for real rays in an ideal aberration-free imaging situation **[shannon 1997]**.

Because of the finite lateral extent of any real optical system, not all the rays which originate at an object point can actually pass through the optical system to form the image. The rays that actually pass through the system are important to determine for two reasons. First, the fraction of light emitted by the object which gets through to form the image determines the brightness of the image. Second, in real systems not all rays can be treated as paraxial rays. Image quality can also be reduced by chromatic aberration. In general, aberrations are caused by differences between where paraxial rays are supposed to go and where actual rays really go. The paraxial rays merely approximate real rays at small slope angles near the optical axis. The paraxial properties of an optical system, such as focal length, depend on the index of refraction; chromatic aberration arises even for strictly paraxial optics **[Ditton 1998]**.

Paraxial rays are very close and nearly parallel to the optical axis. In this region, lens surfaces are assumed normal to the axis, and hence all angles of incidence and refraction are small. As a result, the sine of the angles of incidence and refraction are small and can be approximated by the angles themselves measured in radians. The paraxial formula dose not include effects of spherical aberration experienced by marginal rays which are rays passing through the lens near its edge or margin.

2.2.1 paraxial equations

Figure (2.2) shows a ray of light leaving an object point P and striking the first surface of lens at point P_1 . It is refracted and proceeds to the second surface at point P_2 . The amount of refraction is specified by Snell's law equation (2.7) **[Jenkins 1976]**.

$$n_1 \sin\theta = n_1' \sin\theta' \tag{2.7}$$

where n_1 and n_1' are the refractive indices of different optical media separating by surface, and θ and θ' are the angle of the ray before and after refraction at separating surface. Taylor series of the $\sin\theta$ have the form:

$$\sin\theta = \theta - \frac{\theta^3}{3!} + \frac{\theta^5}{5!} - \cdots\cdots \tag{2.8}$$

where the angle θ is expressed in radians. For very small values of θ, only the first term on the right side of equation (2.8) needs to be used, i.e. $\sin\theta \approx \theta$, equation 2.8 simplifed to:

$$n_1 \theta = n'_1 \theta' \tag{2.9}$$

this is called the paraxial form of the Snell's law, however, the Snell's law angles are not convenient to work with, and eliminate with the identities

$$\theta_1 = u_1 + \phi \tag{2.10}$$

$$\theta_1' = u_1' + \phi \tag{2.11}$$

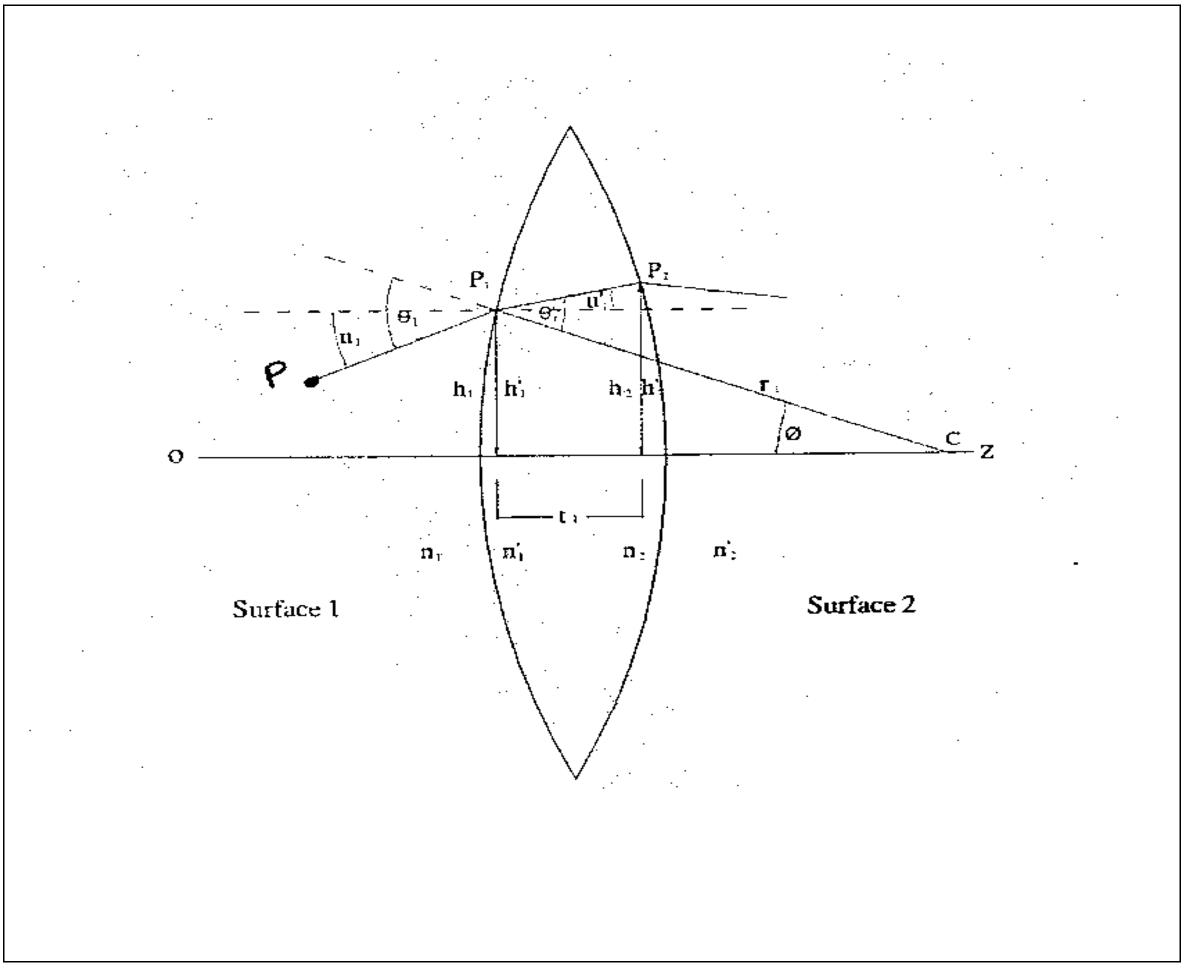

Figure 2.2 shows a ray of light pass through lens surfaces **[Nussbaum 1998]**

where u_1 is the angle of the incident ray, u'_1 is the corresponding angle for the refracted ray, and ϕ is the angle that the radius R_1 of the lens surface makes at the center of curvature Cc. this particular angle can be simplified as

$$\sin\phi = \frac{h_1}{R_1} \tag{2.12}$$

from paraxial approximation one can simplify equation (2.12), to obtain

$$\phi \approx \frac{h_1}{R_1} \tag{2.13}$$

Substituting equation (2.10), (2.11), and (2.13) in to equation (2.9), then we get:

$$n_1' \, u_1' = \frac{n_1 - n_1'}{R_1} \, h_1 + n_1 \, u_1 \tag{2.14}$$

where h_1 is the distance from point p_1 to the axis, P_1 is called the refracting power of first surface and is defined as **[Nussbaum 1998]**

$$P_1 = \frac{n_1' - n_1}{R_1} \tag{2.15}$$

the curvature c_1 of the lens first surface is defined as:

$$c_1 = \frac{1}{R_1} \tag{2.16}$$

Then equation (2.15) may also written as:

$$P_1 = c_1 \, (n_1' - n_1) \tag{2.17}$$

And equation (2.15) written as:

$$n_1' \, u_1' = P_1 \, h_1 + n_1 \, u_1 \tag{2.18}$$

as the ray goes from P_1 to P_2, its height from the axis becomes

$$h_2 = h_1' + t_1 \tan u' \tag{2.19}$$

or, using the paraxial approximation for small angles, we get:

$$h_2 = h_1' + t_1 \, u' \tag{2.20}$$

2.3 Infrared Lenses

Most lenses are made of optical glass in visible portion of the electromagnetic spectrum. Other materials, including crystals, plastics, and reflective substrate materials are important for some applications. Selection of a material for use in a lens design initially requires consideration of the optical properties of the material in addition to its mechanical, physical, and chemical properties. Availability of the material is dependent upon the cost, form of supply, and required working and finishing procedures for the material. A successful optical designer will consider all of the parameters when selecting or recommending materials for a lens **[Shannon 1997]**.

The most important optical property of materials used in lens elements is the refractive index. The refractive index n is defined as the ratio of the velocity of light in surrounding medium and the velocity of light in material, i.e.

$$n = \frac{c}{\upsilon} \tag{2.21}$$

where, most often, the surrounding medium is air. Thus the refractive index is usually stated relative to air. Most optical glass catalogs use this definition of refractive index, selecting standard condition of temperature and air pressure for defining the listed values. Absolute refractive index is referred to vacuum as the surrounding medium, and can be obtained by multiplying the value of index as defined above by the index of refraction of air at standard temperature and pressure. The refractive property of the material is related to the dielectric constant of the material at the frequency of the electromagnetic radiation being transmitted through the material, and is dependent upon the wavelength or color of the light.

In the majority of lens design, materials are required to be homogeneous and isotropic, negligible scattering, and have high transmittance over the desired spectral region.

The index of refraction varies with wavelength. This means that the speed of light in the glass varies with color and this medium is called dispersive. Almost every spectral region of interest, such as glasses, follow a dispersion curve of the form in which the refractive index of the glass is highest for shorter wavelengths.

The properties of the refractive index of the glass are primarily determined by the chemical constituents in the glass, the naming of glass type is meaningful, as all purchases of one type of glass will be of glass that is a member of the same chemical and physical family **[Shannon 1997]** .

Infrared lenses differ from that design for the visual region in several important aspects that may be summarized as follows **[Laikin 2001]**:

(a) There are a fewer materials to choose. Fortunately, available materials such as germanium and zinc selenide have high index of refraction and low dispersion.

(b) Due to the high cost of these materials and their relatively poor transmission, thickness should be kept to a minimum. Many of these materials are polycrystalline and exhibit some scattering which is another reason to keep the lenses thin.

(c) The long wavelength means a much lower resolution requirement.

(d) The walls of the housing emit radiation and so contribute to the background.

(e) Detectors are often linear arrays, in contrast to film or the eye. These detectors are usually cooled.

(f) One must check that the detector is not being imaged back onto itself.

2.4 Aberrations

Aberrations are devations from the perfect geometrical imaging case. Ideal image formation requires that the relation between object and image would follow paraxial rules, and all rays from each object point would pass through its paraxial conjugate image point, with all rays having the same optical path length from object to image. The first-order aberrations are deviations of the Paraxial imaging conditions from the perfect base imagery as determined by tracing ray at a central wavelength. The third, fifth, and so on, orders are aberrations which express a deviation from the paraxially determined imaging conditions **[Shannon 1997]**.

Third-order theory predicts seven types of aberrations. Two of these, called chromatic aberrations. The rest, called monochromatic aberrations. These seven aberrations can be briefly described as follows:

A. Monochromatic Aberrations

Its occur even though only a single wavelength is involved **[Hudson 1969]**. For a monochromatic light ray aberrations arise due to geometrical deviations from paraxial (Guassian) theory. First order theory correspond to the approximation $\sin\theta \approx \theta$ in radians. If the approximation is extended to the next term, one can predict deviation from paraxial theory when $\sin\theta = \theta - \theta^3/3!$. This third order theory describes the five primary monochromatic or Seidel Aberrations which are discuss as follows **[Physics 1998]**:

i. Spherical aberration

Spherical aberration is defined as the variation of focus with aperture, where aperture means the diameter of the section of the lens used to form the image **[Nussbaum1998]**.

The spherical aberration is the first of the five Seidel aberrations, and usually one must correct this aberration before attempting to reduce the others. Figur (2.3) shows the spherical aberration for lens. From Figure we see that the distance between the marginal and paraxial focal plans is called longitudinal spherical aberration (LSA), while the distance between the points where the rays cross the paraxial focal plane is called transverse spherical aberrations (TSA) **[Donald 1985]**.

Longitudinal spherical aberration (LSA) and transverse spherical aberrations (TSA) are not independent of each other since they are related by the marginal convergence angle.

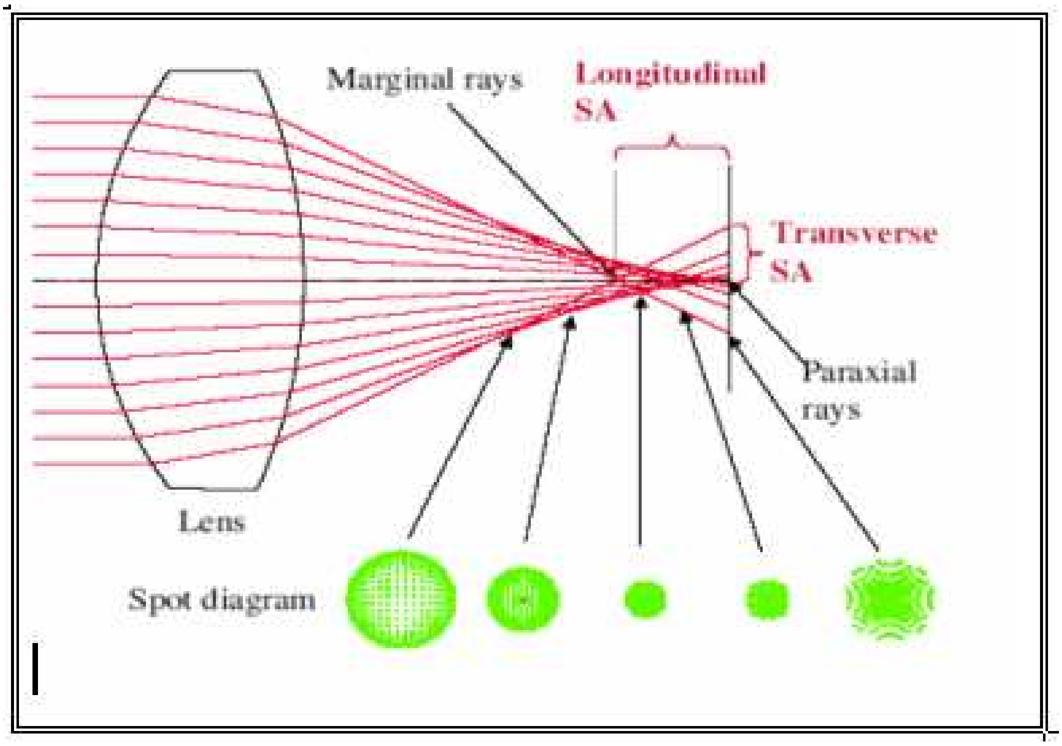

Figure 2.3 Spherical aberration for lens **[Nussbaum 1998]**

ii. Coma

Figure (2.4) shows comatic aberration which is similar to spherical aberration. It applies to rays entering the lens at an angle i.e. it indicates an off-axial aberration that is non-symmetrical about the optical axis and increases with the radius of the lens aperture. The focal point of the lens will vary the further away the ray hits the lens from the centre. Due to this, image blurring is found the further off-axis one goes. A single lens can be shosen that will give no coma but only at a set distance from the object one would like to image **[Jenkins and White 1976]**.

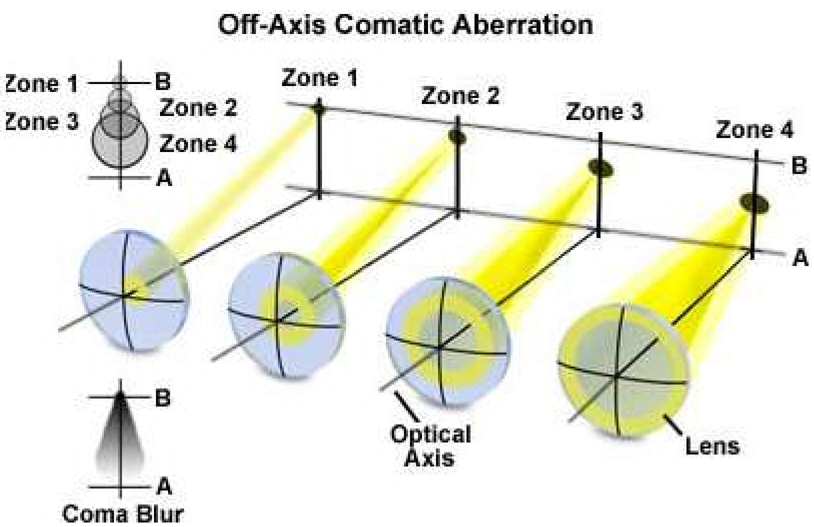

Figure (2.4) The geometrical coma of a point **[Hecht 1998]**

iii. Astigmatism

Astigmatism arises since an object point is a distance from the optical axis then the cone of rays from that point will strike the lens asymmetrically. In other words the focal length of the lens will vary depending on where the rays hit the lens. This will lead to rays which are less parallel to the optical axis being focused differently from those which are parallel or almost parallel to the optical axis as shown in figure (2.5). This means that for some points the object will always be blurred as while one can focus the light for some of the rays one cannot focus it for all of them **[Jenkins and White 1976]**.

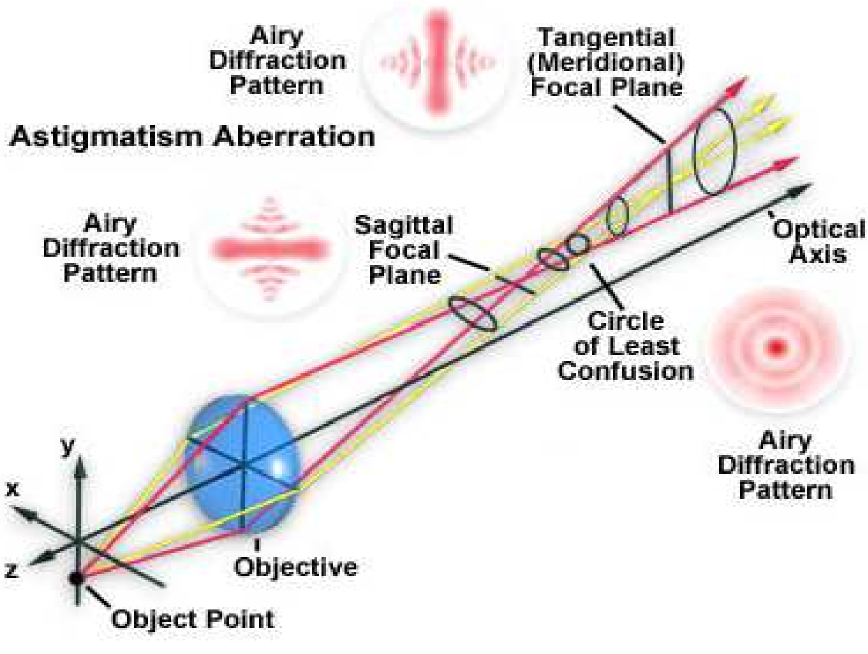

Figure 2.5 Astigmatism aberration **[Hecht 1998]**

iv. Curvature of Field

For rays entering the lens on or near the optical axis (paraxial rays), the focal length of the lens (barring other aberrations) is constant. This leads to the problem of field curvature. As the distance from the centre of the lens to the focus point is constant then the image of a plane object described by the lens is going to be on a curved rather than on a plane surface as illustrated in figure (2.6) **[Hecht 1998]**, the curvature increases with the off-axis distance of the object and with the aperture of the lens **[Jenkins and White 1976]**.

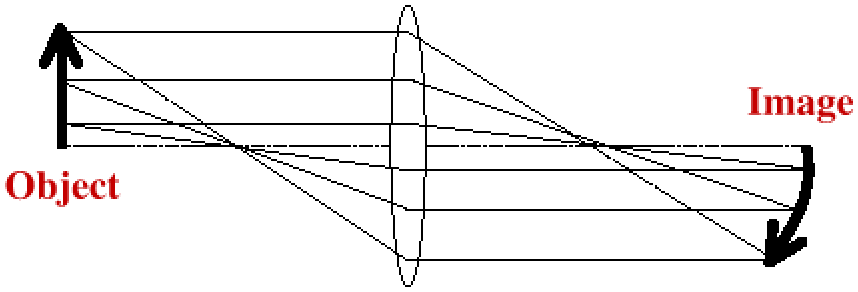

Figure (2.6) The field curvature is mainly visible at the edges of the field **[Hecht 1998]**

v. Distortion

The focal length of the lens and hence the magnification will cause varies over the surface of the lens (i.e. a ray hitting the lens at one spot while be focused more or less than that at another). This leads to distortion. Distortion is where parts of the image are magnified more or less than others. The most common distortions are barrel distortion (where the centre of the image is bigger than the edges) and pincushion distortion (where the edges are bigger than the centre) as shown in figure (2.7) **[Hecht 1998]**. The image, in other case, is sharp but distort. These can commonly be seen on television's screen and computer's monitor **[Jenkins and White 1976]**.

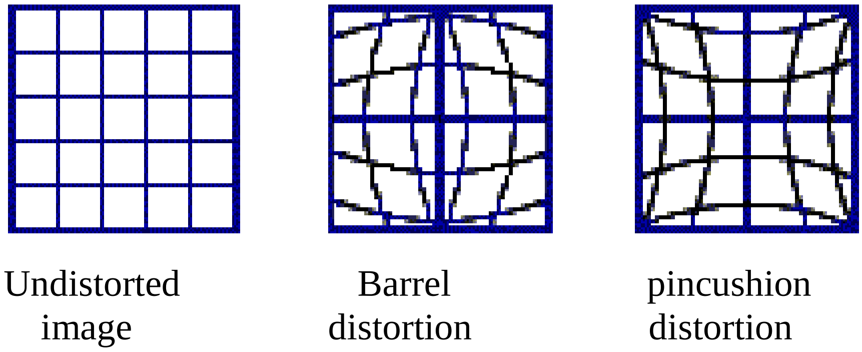

Figure (2.7) The distortion aberration **[Hecht 1998]**

B. Chromatic Aberrations

Chromatic aberrations, are caused since the index of refraction varies with the wavelength of light, the properties of optical elements also vary with wavelength. There are two types of chromatic aberration:

i. Longitudinal: A variation of focus (image position) with wavelength. In general the index of refraction of optical materials is higher for short wavelengths than for long wavelengths, as shown in figure (2.8) **[Welford 1974]**.

ii. Lateral: The size of an image formed by the optics varies as a function of wavelength **[Hudson1969]**.

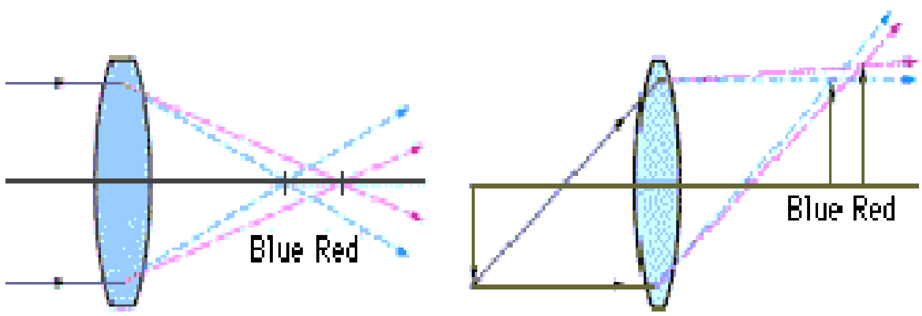

Figure (2.8) Chromatic aberration **[Aberration and Distortion 2005]**

2.5 Optical Invariants

It is important to mention the optical invariants before introducing Seidel aberration formulae because the forms of the optical invariants are implanted in the primary aberration theory by the symmetry of the expressions of the barred and unbarred quantities as shown below. The barred quantities are those belong to the principle ray (figure 2.9).

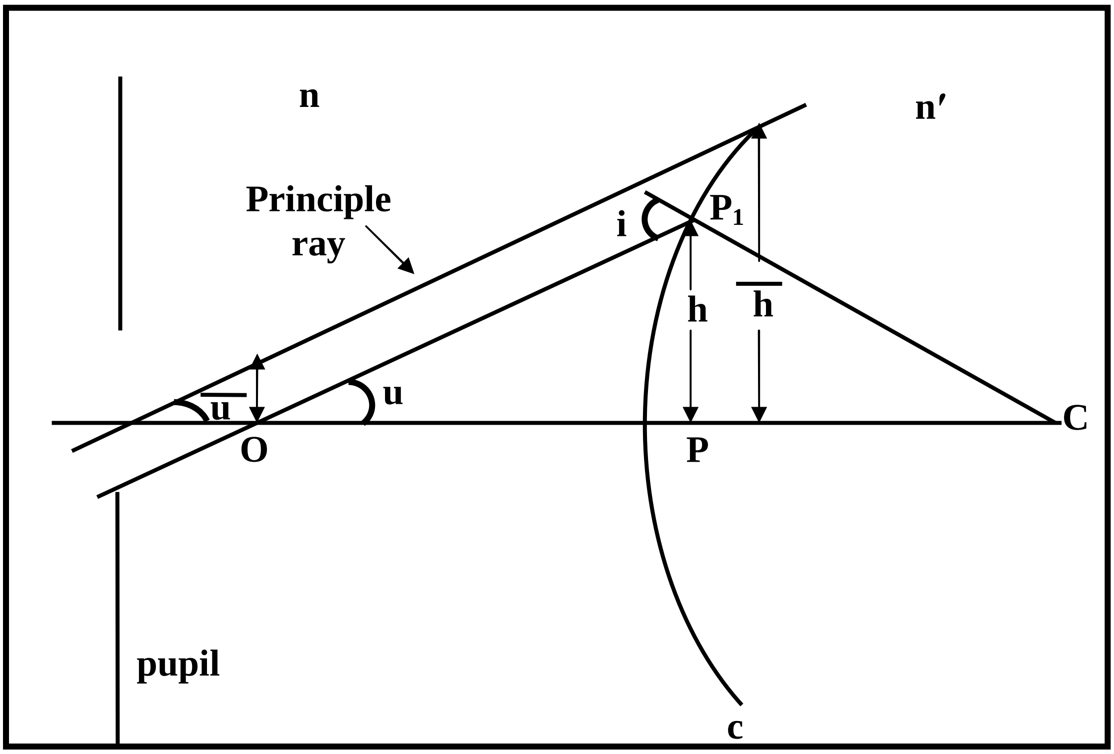

Figure (2.9) The optical invariants

From figure (2.9), let O be the axial object point, P the axial point of the refracting surface, C the centre of curvature of the refracting surface and P_1 the point of incidence of the paraxial ray through O which touches the rim of the pupil. Then in paraxial approximation hc is equal to the angle of convergence OCP_1 and thus, in the triangle OCP_1 the external angle at P_1 is given by hc+u, this is the paraxial angle of incidence, which is denoted by i, so it is found that **[Welford 1974]**:

$$i = hc + u \tag{2.22}$$

and from Snell’s law one get:

$$n\left(hc + u\right) = n'\left(hc + u'\right) \tag{2.23}$$

For simplicity, we denote that

$$A = nu + nhc \tag{2.24}$$

and

$$\overline{A} = n\overline{u} + n\overline{hc} \tag{2.25}$$

Consider figure (2.10) which represent the case of Gaussian system.

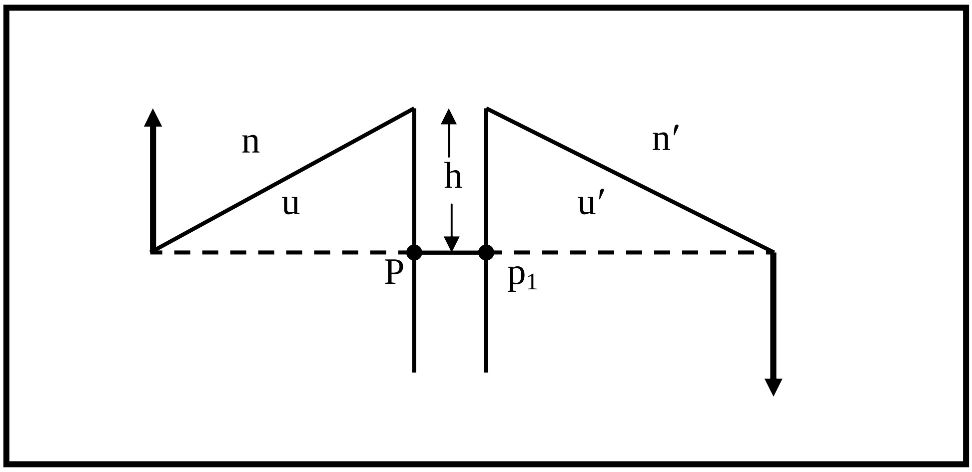

Figure (2.10) Transverse magnification

The form of the Gaussian formation image can be express as:

$$nu\eta = n'u'\eta' \tag{2.26}$$

where η'/η represents the transverse magnification. Equation (2.26) has a much wider application than to the calculation of transverse magnification. The right hand side quantity $n'u'\eta'$ for the first system while $nu\eta$ represent the second hand side, i.e., the image of the first system will be the object of the second and so on. Thus, this quantity is invariant through both systems and, therefore, it must be an invariant right from the object space through all intermediate spaces of any symmetrical optical system. This invariant is known as the Lagrange invariant and denoted by "H" **[Welford 1974]**.

The Lagrange invariant, as a part of the structure of Gaussian optics, has a much wider application than to the calculation of transverse magnification (equation 2.26). it is significant in photometry of optical instrument, since H^2 represents in the Gaussian approximation the total light flux through a given transverse section of an optical and its invariance through a system is therefore a consequence of the conservation of energy. Also, the Lagrange invariant divided by the wavelength of the light is the unit in the dimensionless coordinates used in the diffraction theory of optical instruments. Another importance of the Lagrange invariant gives rise from calculating the primary aberration **[Welford 1974]**.

From equation 2.26 H can be written in terms of the ray tracing data (u and h) as **[Welford 1974]**.:

$$H = n\left(u\,\bar{h} - \bar{u}\,h\right) \tag{2.27}$$

When u goes to zero, in this result the form of the Lagrange invariant is for a star space. Since $\bar{u}$ is now the field angle. From equations (2.28) and (2.29), one can write H in terms of refraction invariants as **[Welford 1974]**:

$$H = A\bar{h} - \bar{A}h \tag{2.28}$$

The forms of Lagrange invariant given in equations (2.26) to equation (2.28) have the merit that they make explicit connection between the ray through the center of the object and the ray through the center of the pupil (principal ray). In other words, if the path of one paraxial ray through an optical system is known, then the path of any other ray can be found from it without need for a new paraxial ray tracing. The first one who made use of this essential point was Seidel who calculate the primary aberration .

To obtain the data of ray tracing **(** $\bar{u}$ and $\bar{h}$ **)** of the principal ray, the term E, sometimes called Seidel eccentricity since it gives a measure of $\bar{h}/h$ (the relative displacement from the axis of the center of the image-forming pencil at the current refracting surface), should be used since it is expressed in terms of the paraxial ray as **[Welford 1974]**, and therefore equation 2.28 can be written as:

$$\bar{h} = hHE \tag{2.29}$$

using in equation (2.28), yields

$$\bar{A} = \frac{A\bar{h} - H}{h} \tag{2.30}$$

2.6 Seidel Aberration and Sum Expressions

Seidel was formulated five sum expressions to calculate the primary aberration in terms of the data of the praxial ray (u and h), and the optical invariance given by (2.19), (2.21), (2.24), and (2.25). The five sum expression are S_I, S_{II}, S_{III}, S_{IV}, and S_V are as follow **[Welford 1974]**:

$$S_I = -\sum_{all\ surface} A^2\ h\,\Delta\left(\frac{u}{n}\right) \tag{2.31}$$

$$S_{II} = -\sum_{all\ surface} \bar{A}A\,h\,\Delta\left(\frac{u}{n}\right) \tag{2.32}$$

$$S_{III} = -\sum_{all\ surface} \overline{A^2}\ h\,\Delta\left(\frac{u}{n}\right) \tag{2.33}$$

$$S_{IV} = -\sum_{all\ surface} H^2\,c\,\Delta\left(\frac{1}{n}\right) \tag{2.34}$$

$$S_V = -\sum_{all\ surface} \left\{\frac{\overline{A^3}}{A}\,h\,\Delta\left(\frac{u}{n}\right) + \frac{\bar{A}}{A}H^2\,c\,\Delta\left(\frac{1}{n}\right)\right\} \tag{2.35}$$

where S_I is the Seidel spherical aberration, S_{II} is coma aberration, S_{III} is astigmatism aberration, S_{IV} field curvature aberration, and S_V is the distortion aberration.

These expressions enable the designer to make modifications to his design, since they involve some degrees of freedom (the refractive indices, and curvatures) to minimize aberrations, and the symbol Δ refers to the change of the quantities enclosed by the parentheses **[Welford 1974]**.

2.7 Spot Diagrams

when a system of rays originally at a single object point is constructed, so that the rays are uniformly distributed over the entire entrance pupil, the plot of their consequent intersecions with the image plane is called a spot diagram. An experienced designer looking at this particular diagram would probably recognize considerable vignetting and coma in the optical system. The size of spot diagram shows the designer the extent of the energy distribution and the shape is due to the type of aberration. When the spot diagram has been reduced to a size comparable to that of the central fringes in a diffraction pattern, a ray theory ceases to be as useful as wave theory **[Williams and Becklund 1986]**.

The spot size is an important parameter since it determines the optical system efficiency. Theoretically, the following relationship gives the size of the spot formed by a single lens under free aberration condition. The diameter of the first dark ring of the Airy rings is given by equation (2.3).

In one deals with a usual optical system, some modifications should be imposed on equation (2.3) to correct the computed spot size formed by the optical system. The modification includes the addition of an spherical aberration term. Hence, the size of the spot formed by an optical system can be calculated from the following equation **[Scott 1959]**.

$$Spot\ size = 2.44\,\lambda\,(f/\#) + \frac{T\ f}{(f/\#)^3} \tag{2.36}$$

where T is a constant given by the following expression **[Scott 1959]**,

$$T = \frac{n+2}{n(n-1)^2} B^2 - \frac{4(n+1)}{n(n-1)} B + \frac{3n+2}{n} + \frac{n^2}{(n-1)^2} \tag{2.37}$$

and $B = \dfrac{r_2 + r_1}{r_2 - r_1}$

where B is the shape or bending variable, n being the refractive index of the last surface, and r_1 and r_2 are the radii of the lens.

2.8 The Modulation Transfer Function (MTF)

The resolution and performance of an optical system can be characterized by a quantity known as the modulation transfer function "MTF", which is measurement of the optical system ability to transfer contrast from the specimen to the intermediate image plane at a specific resolution. Computation of the modulation transfer function is a mechanism that is often utilized by optical manufactures to incorporate resolution and contrast data into a single specification **[Davidson 2006]**.

A perfect optical system would have a modulation transfer function of unity at all spatial frequancies, while simultaneously having a phase transfer factor of zero.

When a specimen is observed in an optical system, the resulting image will be somewhat degraded due to aberrations and diffraction phenomena, in addition to minute assembly and alignment errors in the optics. In the image, bright highlights will not appear as bright as they do the speciment, the dark or shadwed areas will not be as black as those observed in the original pattens.

By convention, the modulation transfer function in normalized to unity at zero spatial frequency. Modulation is typically less in the image than in the specimen and there is often a slight phase displacement of the image relative to the specimen. By comparing several specimens having differing spatial frequencies, it can be determined that both image modulation and phase shifts will vary as a function of spatial frequency. By definition, the modulation transfer function is described by the equation:

$$\text{MTF} = \frac{\text{Image Modulation}}{\text{Object Modulation}} \tag{2.38}$$

This quantity, is an experssion of the contrast alteration observed in the image of a sinusoidal object as a function of spatial frequancy **[Davidson 2006]**. Figure 2.11 shows the change of MTF with spatial frequancy for the perfect limit diffraction.

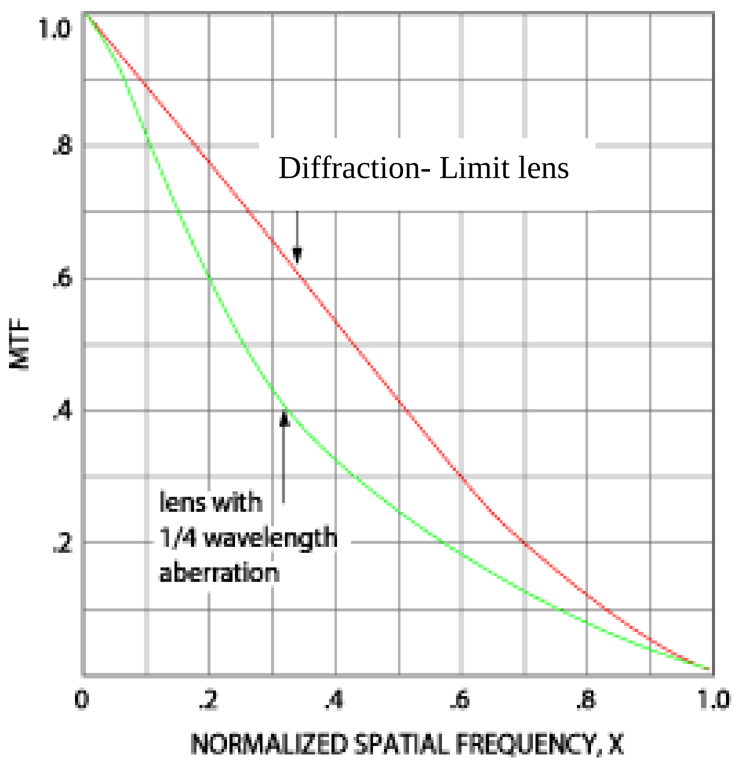

Figure 2.11 MTF as a function of normalized spatial frequency

CHAPTER THREE

OPTICAL DESIGN OF A HOMING HEAD SYSTEM

3.1 Introduction

The optics used in an infrared missile-seeker (homing head) result from a series of design compromises involving sensitivity, resolution, and geometry.

The sensitivity, S, of such IR systems varies, in general, with the aperture diameter "D", optical efficiency "e", and the ratio of focal length to aperture diameter i.e. F-number, $F^{\#}$, i.e. : $S \ \alpha \ De / F^{\#}$ **[Dubner 1959]**.

Figure 3.1 shows the homing head configuration of an IR missile-seeker used in the present work. The folded optical system consists of dome, primary mirror, secondary mirror, and correcting lens. A brief description of the major elements of an IR homing head is as follows **[Dubner 1959]**:

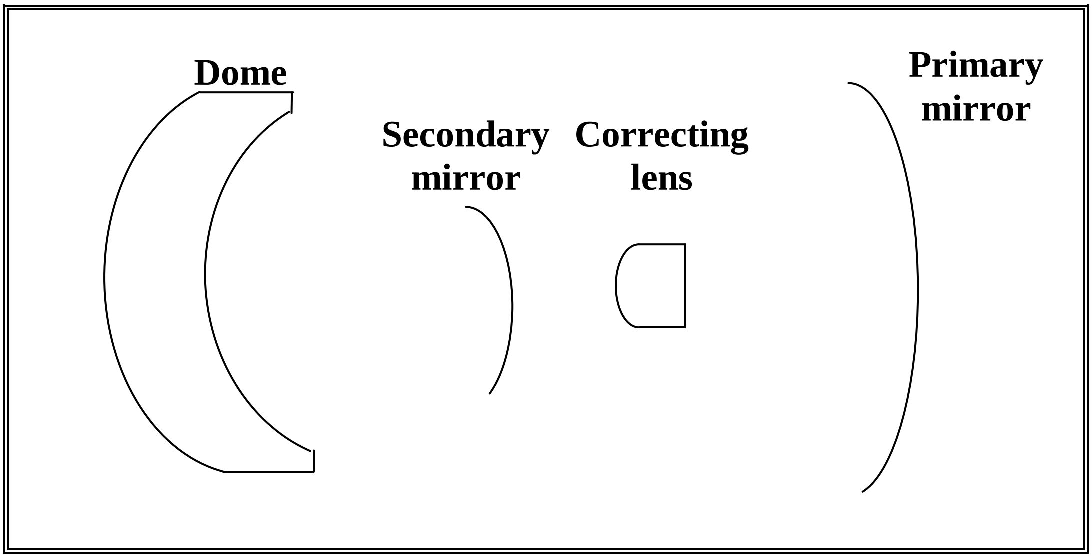

Figure (3.1) Optical system design for IR homing head.

A. Dome

The dome introduces spherical aberration opposite to that of the primary mirror. It also produces significant amount of higher-order on-axis aberrations. It is interesting to note that although the paraxial power of the dome is equal and opposite to that of the mirror, this means that the dome is a highly nonlinear element with high aberration. In optical terms, the principal ray of the system is perpendicular to the dome surface so that almost no off-axis aberrations are generated by the dome.

Befor the selection of a material there are certain requirements which must be met. The window, either flat plate or dome, must withstand the flight profile stated for its application. The mechanical properties should be strong enough to prevent catastrophic failure.

The likely cause of this would be cracking and fracturing due to the thermal and stress loads imposed on the window during the first five seconds of flight. This is the critical time for the build up of stress and external temperature. A high temperature differential between external and internal surfaces may induce thermal stress leading to cracking. This will not be so great a problem if the material has a high thermal conductivity.

B. Primary Mirror

The primary mirror introduces spherical aberration, coma, and astigmatism. This element is used as the aperture stop. In attempting to improve the resolution, the first logical step was to investigate the use of a more complicated primary mirror. This was done by using thin-lens formulas. A study of a mangin (back surface) mirror showed that by keeping the power of the lens constant and just bending the lens, the astigmatism remains constant, the coma decreases, and the spherical aberration decreases through zero and then increases negatively. If this mirror were used to correct coma, the spherical aberration would have reversed sign, and the dome would no longer be able to correct the residual spherical aberration. Therefore, a correcting lens is required to cancel the remaining spherical aberration.

C. Secondary Mirror

Using thin-lens formulas, an investigation was made on a mangin secondary mirror. The system is composed of the primary mirror and a mangin secondary mirror. The optical aberration varies rapidly as a function of lens bending. At the point where spherical aberration is near zero, the mangin secondary mirror behaves in much the same manner as the dome; that is for large changes in spherical aberration there is little change in either coma or astigmatism. Thus, a dome can now be chosen independent of the spherical aberration required; the mangin mirror can supply the residual spherical aberration.

D. Correcting Lens

Since both the mangin primary and the mangin secondary mirrors required a correcting lens in front of the focal plane, a thorough analysis was made of a system consisting of a dome glass, a primary mirror, a secondary mirror, and a lens. The first objective was to find a configuration which would zero coma. It was found that particular lens power, the lens can be bent so that there is no coma. For zero coma, astigmatism, and spherical aberration were function of lens power.

3.2 Materials of the IR Optical System

The following is brief description of the materials that are used in IR optical systems.

i. Germanium (Ge)

Germanium is most widely used for lenses and windows in IR systems operating in the 2-12 μm range. Enviroment dose not make any problems because Germanium is inert, mechanically rugged, and fairly hard. It is an excellent choice for multi-spectral systems and for applications where EMI shielding is necessary. Germanium can be electrically heated for anti-fogging or anti-icing applications **[Optical Materials 2005]**.

ii. Sapphire (Al_2O_3)

Sapphire is a single crystal aluminum oxide (Al_2O_3). It is one of the hardest materials. Sapphire has good transmission characteristics over the visible, and near IR spectrum. It exhibits high mechanical strength, chemical resistance, thermal conductivity and thermal stability. It is often used as window materials in specific field such as space technology where scratch or high temperature resistance is required **[Optical Material 2005]**.

iii. Calcium Fluoride (CaF_2)

Calcium fluoride is used for optical windows, lenses and prisms in 0.15-9 μm range. Because of its low absorption at wavelength shorter than 6 μm, CaF_2 is particularly popular for high power laser optics in that wavelength range. Due to its low refractive index it can be used without anti-reflection coating **[IR Materials]**.

iv. Lithium Fluoride (LiF)

Lithium fluoride has the lowest index of refraction of all the common infrared materials. LiF is slightly plastic, and has a relatively high thermal expansion coefficient. It is also the most expensive of the Fluoride series of crystals **[Optical Materials Selection Guide]**.

v. Magnesium Fluoride (MgF_2)

Magnesium fluoride is the only optical material combining wide spectral transmittance band with birefringence phenomenon and satisfactory thermal expansion coefficient for isotropic cross section. It is used for UV-radiation sources and receivers windows manufacture; for optical elements of interference-polarization filters, as laser resonator optics elements in quantum electronics and as active material in IR and sub millimeter band **[Optical Material 2005]**.

vi. Barium Fluoride (BaF_2)

Barium fluoride crystals are transparent in wide spectrum band. The product finds use in windows, lenses of special types of objectives, as mirrors substrate in optical systems operating in UV and IR spectrum band **Optical Material 2005]**.

vii. Sodium Chloride (NaCl)

Sodium chloride is used for lenses where transmission in the (0.25 – 16) μm range is desired. Because of its low absorption, Sodium Chloride is being used in high power laser systems. Polished surfaces must be protected from moisture by exposing to only dry atmosphere or by using a heating element to maintain the Sodium Chloride above the ambient temperature. Sodium Chloride can be used up to 400° C. The material is sensitive to thermal shock. Irradiation generates color centers **[Optical Materials 2005]**.

Table (3.1) shows the refractive index for 4 μm wavelength transmission range, and coefficient expansion for different materials.

Table (3.1): Selected materials for the 3-5μm spectral band **[ISP Optics 2005]**.

Optical Materials	**Refractive Index for 4 μm**	**Transmission Range (μm)**	**Coefficient Expansion /C°** β(*10^{-6})
Germanium (Ge)	4.025	2.0 – 14.0	5.7
Sapphire (Al_2O_3)	1.6679	0.17 – 5.0	6
Sodium Fluoride (NaCl)	1.5217	0.2-20	44
Barium Fluoride (BaF_2)	1.4558	0.15 to 12.5	18
Calcium Fluoride (CaF_2)	1.410	0.130 - 7.0	19
Magnesium Fluoride (MgF_2)	1.349	0.130 - 7.0	12
Lithium Fluoride (LiF)	1.3494	0.121 - 5.0	37

CHAPTER FOUR

RESULTS AND DISCUSSION

4.1 Design Considerations

Optical design of a homing head system used in infrared applications fields has been put forward with aid of ZEMAX program. The suggested system consist of refracting and reflecting components in order to expand or compress a beam of light. Optical system design has its own advantage and disadvantages concerning, for instance, its fabrication process, simplicity, compatibility, and cost.

Figure (4.1) shows the suggested optical design for infrared homing head system which is used in our work. The system consists of dome, primary mirror, secondary mirror, and correcting lens. The selection of materials operate in the range (3-5) μm region of the spectrum the optical system has been studied. Some of commonly used materials for this region are listed in table (3.1).

The computational work passes through two stages. The first stage is improving the optical system design. The improvement is done by changing the materials of the correcting lens and dome, with materials have an additional characteristics related by its plentifulness and industrialization technique.

The second stage is a descriptive investigation utilize to choose the optical parameters that describe the performance of the suggested optical system design.

In the present investigation Zemax has been used to determine the design of the optical systems for the IR homing head.

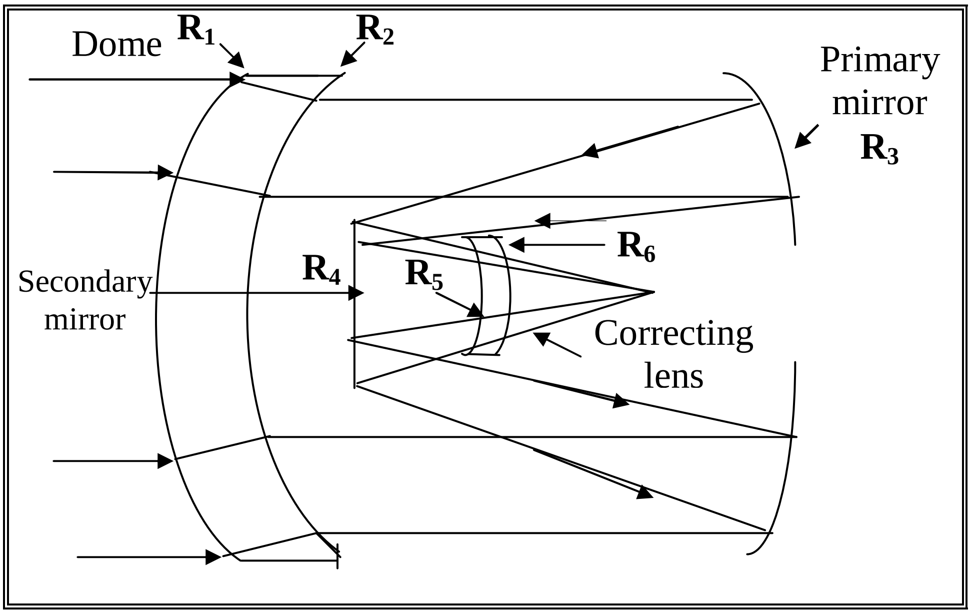

Figure (4.1) Optical system design of IR homing head

4.2 Choice of variables

Any parameter describing the lens could be used as a variable. Usually only a subset of the available is used in order to maintain some control over the properties and configuration of the lens. The most important variables are the curvature of the surfaces. Usually the designer will elect to use the "radius of curvature ", which is easier to visualize, as it is physical quantity that will be measured in building the lens **[Shannon 1997]**.

The other type of variable is the separation between optical surfaces. This can be the thickness of element, or air space between the elements (air lens). In some cases, thickness can be infinitesimal, indicating that the two surfaces of lenses are contact or cemented. In general, if left unbounded lenses will usually expand to fill all of the available space during a design. Therefore, the thickness variables should always be bounded **[Shannon 1997]**.

The optical properties of the materials used in a lens can obviously be variable. Usually the optical glasses used will be established at the beginning for cost, delivery, and environmental reasons. The materials must be replaced by the closest available material and optimization run completed with specified material in order to have a physically viable lens **[Shannon 1997]**.

In the present work, the conventional design have been modified. The modification have been done by using different materials for the dome and correction lens. These materials have closest properties to the used conventional one, used in the spectral region which is in (3-5) μm.

The best radii of curvatures of the correcting lens of optical system R_5, and R_6 are choose by using optimization method. In our work, the thickness of dome, and correcting lens are assumed to be constants.

4.3 Image Quality Evaluations

Two effective parameters have been taken into account which describe the efficiency of the optical system on image quality. These parameters are:

A. Spot size

All light rays cross the optical axis at a single point, forming a spot with a diameter determined by the diffraction formula given by equation (2.3). The point spread function "PSF", determine the energy distributed on the image plane due to a point source located on the object plane **[Donald 1995]**. Many lenses exhibit a phenomenon termed spherical aberration. Spherical aberration has the effect of increasing spot size given by equation (2.36).

B. Modulation transfer function

MTF is one of the most important parameters determines the efficiency of the optical system. MTF is very sensitive to many different types of aberration. It may be described by a set of points as a function of frequency. A plot of this sort has a maximum value at zero frequency. The relations refer that the maximum of this curve is unity; therefore, i.e. it is normalized curve. In other words, MTF values corresponding to a specific value of frequency in the MTF curve represents the percentage of the optical system design to receive the information at that frequency. Therefore, the MTF value corresponding to a specific frequency indicates the amount of image contrast relative to the object contrast.

Analytically, if one deals with a perfect optical system design then the image will have a specific contrast and the behavior of MTF distribution depends on the frequency and its curve will decrease with increasing frequency until it reaches a zero value at the cutoff frequency. The computed Figure (4.2) shows the MTF curve for a perfect optical system (aberration free system).

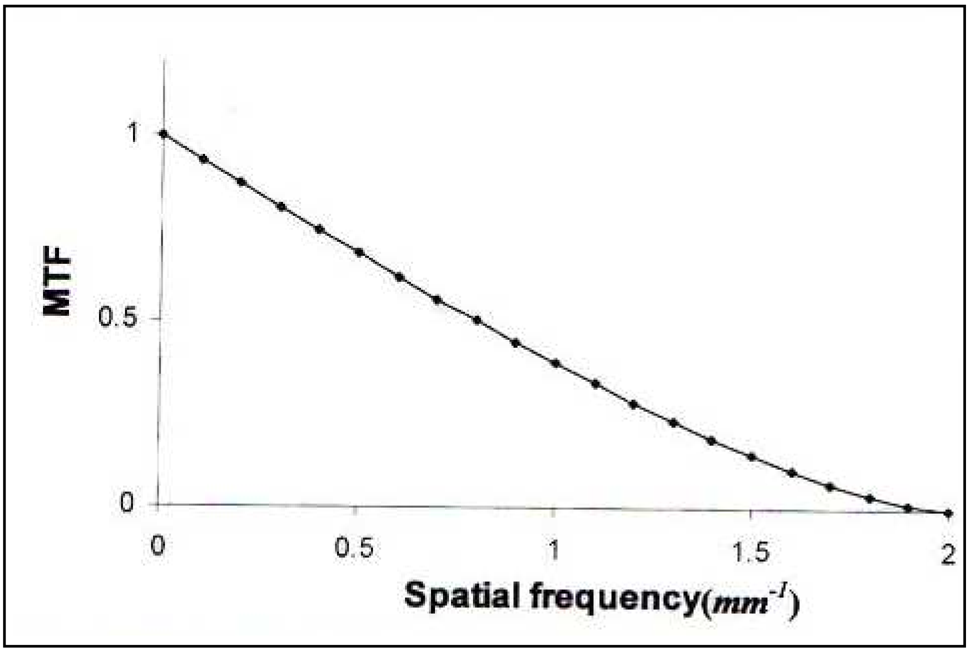

Figure 4.2 Perfect MTF

When an optical system has some aberration, its MTF curve will be different from that of the perfect one by its slope and behavior, especially in the high frequency region, where the amount of the decay will increase and is proportional to the aberration. The signal in this region diffused with the background noise since both of them have same frequency, which interpret the oscillations occurred in the high frequency region.

In order to show the variation of MTF with the aberration, the amounts of aberration and defocusing agreed previously have been considered. Figure (4.3) shows the behavior of the MTF compared with the perfect MTF for different amounts of aberration and defocusing, which prove the great sensitivity of the MTF curve to the aberration and defocusing. It is seen that the curve of the middle case is the best since it near to the perfect case. Also, the defocusing affect the decay of the MTF curve, while the aberration affect the smooth behavior of the MTF curve.

4.4 Results

Table (4.1) shows the abbreviation OBJ, STO, and IMA listed in surface column represent the object, stop aperture, and image respectively. It should be mentioned that in the IR lens object indicates for IR rays coming from target, the stop aperture located in primary mirror and the image represent the spot on the detector.

Table 4.1 Optical data of standard design (all dimensions are in millimeter)

Surface	Radius	Thickness	Glass	Semi-Diameter
OBJ	Infinity	Infinity	air	0
1	40	4	MgF_2	17.5
2	32.77	32	air	16.94105
STO	-84.5	-30	Mirror	17.953298
4	-141	7.15	Mirror	6.447437
5	46.88	1.8	Sapphire	4.167998
6	-115.8	8.97325	air	3.838856
IMA	Infinity		air	0.121891

The radius column in table (4.1) represents the radius of curvature of a lens. Infinity indicates for a plane surface i.e. a surface whose radius of curvature is infinity. The minus (-) and plus (+) signs indicate for a concave and convex surface, respectively for the lens under consideration.

Thickness column represent thickness of each optical element and separation between that elements (air lens thickness).

Glass column contains the type of glass materials used in the lens design process. The blanks in this column indicate that region is occupied by air lens.

Semi diameters in table (4.1) refer to the value of the lens aperture radius in millimeters.

The dome is meniscus lens used to separate the received radiation on the face of the second element (primary mirror). The material of the dome is MgF_2, which have a desirable optical properties.

The primary mirror is a concave one which is used for receiving the radiation traversing the dome and deliver them to the surface of the third element (secondary mirror). It may also be used to reduce the spherical aberration. The function of the optical system is highly affected by the distance between primary mirror and the dome. The computations have shown that increasing the dome-primary mirror distance will give rise to closer angles of reflection for the off-axis and paraxial rays; thus better focusing will be achieved. Therefore, one can say that a high quality spot depends, among other parameters, on the distance between the dome and the primary mirror. However, there is a limitation to this distance. A short distance requires a high radius of curvature for the primary mirror to enable the rays to be collected on the surface of the secondary mirror.

The secondary mirror is a convex one where the radiation coming from the concave mirror are reflected to be collimated by the fourth element which is the correction lens. The function of this mirror is to bring back the radiation towards their original direction at a higher density and close to the optical axis. A small radius of curvature of the secondary mirror will increase the reflection angles of the rays which are collected in the vicinity of the secondary mirror that makes focusing on the detector rather difficult. However, a secondary mirror of large radius of curvature will make the rays to be collimated on the optical axis far from the mirror due to angles of reflection. This case would require that the secondary mirror should be followed by a correction lens of the double convex type with large radii of curvature.

The double convex correction lens is the fourth element in the optical system. It has an important role in the focusing process. The value of radius of curvature should be such that the emerging rays are collimated vary close to the optical axis.

Table 4.2 Data of General lens.

Number of surfaces	8
Stop	4
Lens units	Millimeter
System aperture	Entrance pupil
Glass catalog	Schott Infrared
Effective focal length	45.32924
Back focal length	8.97325
Total track	36
F-number F/#	1.329849
Numerical aperture NA	0.3601563
Stop radius	17.97072
Entrance pupil diameter	35
Wavelength	3-5 μm
Field of view	0

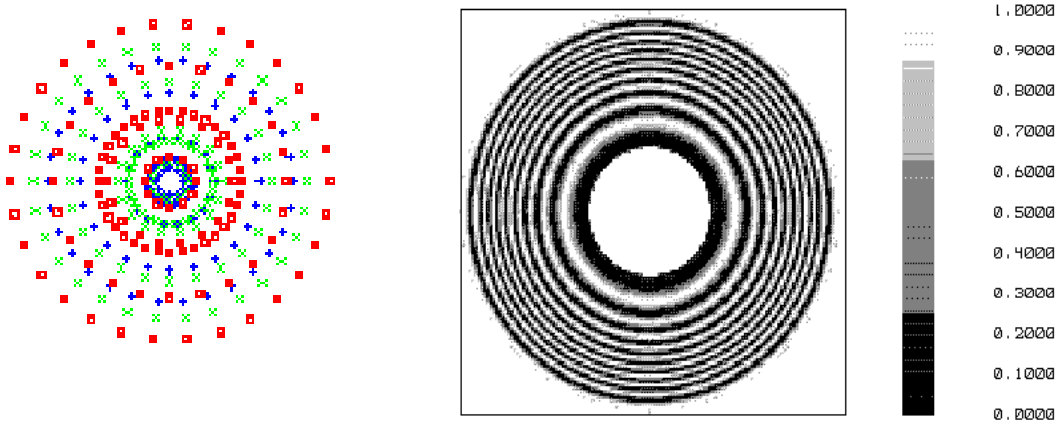

(a) spot grey pattern for the suggest design

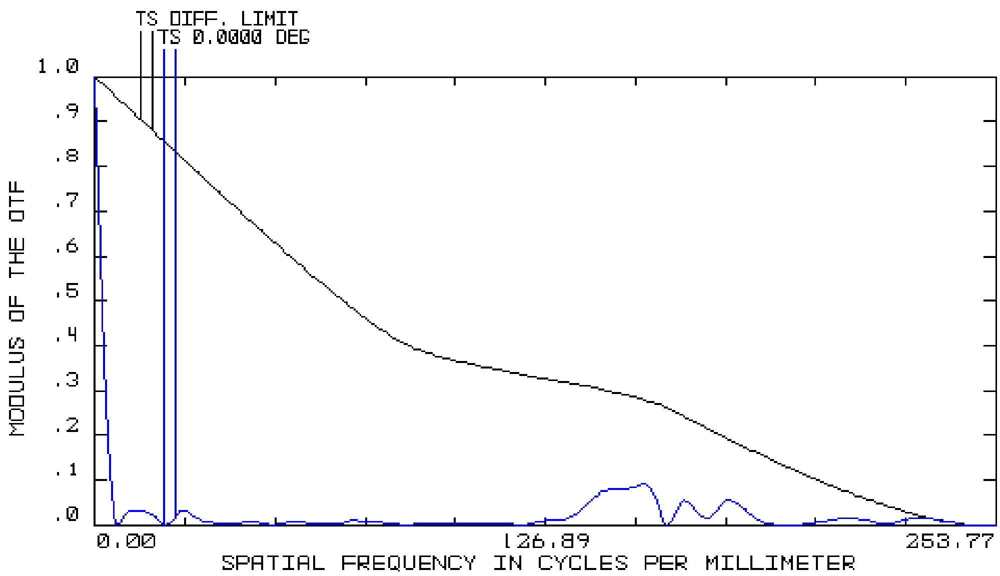

(b) Normalized modulation transfer function (MTF) for the suggested design

Figure (4.4) Result of suggested design before correcting the aberrations

The processing of aberration is a very important task in the optical system design, since its of high effect on the image quality. Only the correction part have been adopted to reduce the optical aberration. In the present work, only the spherical aberration and defocusing have been taken into account whereas other type of aberrations have been neglected due to their little effect on the image quality. Moreover, the spherical aberration and defocusing are reduced by changing the features of some optical element in correcting part, in order to bring them to the lowest possible value.

Zemax software has been used to present the behavior of the effective parameters corresponding to different amounts of spherical aberration. These aberrations are created by changing the radius of curvature of the correcting lens.

A trial and error method has been adopted in order to achieve the lowest possible spot size and the associated aberrations. The smallest size of spot requires solution of the following two important problems in order to achieve high resolution:

(i) Reducing spherical aberration to the lowest possible value which is the task of the correction.

(ii) Good focusing by the system elements which is the task of the collection part.

The process begins by varying R_5 and R_6 while the thickness of the correction lens is assumed to be constant. The method is repeated for different refractive index of the correcting lens material as shown in table (4.3).

The analytical consideration is to show what are the effective parameters that can provide complete indication about how efficient the suggested optical system design. Since the function of the optical system design of an IR homing head is to detect and track a distance object, the accuracy of the calculations is very important. In order to achieve high accuracy, an analytical study on how to determine the effective parameters of the optical system has been performed. The analysis includes a test for some of well-known optical functions at different amounts of aberration and defocusing, then studying their behavior and how they are affected.

Table 4.3 Spot size, Seidel spherical aberration, and the corresponding optimized radius of curvature $R_5$and R_6 for **MgF_2** dome's material.

Materials of correction lens	**R_3 (mm)**	**R_4 (mm)**	**Spot size Radius (μm)**	**Si**
Germanium (n = 4.025)	-47.25	-37	87.32	0.04134
Sapphire (n= 1.667)	-115.16	-28	43.143	0.03986
NaCl (n = 1.5217)	Infinity	-27.8	88.842	0.04111
BaF2 (n = 1.455)	152.5	-28.05	85.692	0.04186
CaF2 (n = 1.41)	78	-28	74.837	0.04345
MgF2 (n = 1.349)	41	-28	63.471	0.04446
LiF (n = 1.3494)	41	-28	46.517	0.0447

Table (4.3) shows that the Sapphire correction lens, which is a convexo-concave lens, give a better results, i.e. gives minimum values of Seidel spherical aberration and radius of spot size. After changing R_5 and R_6 we get that the spot radius is 43.143μm with such small Seidel spherical aberration equal to 0.03986.

Figure (4.5) shows the result of image quality after correcting the aberration. From Figure 4.5.a we conclude that we get better spot since it have a high intensity with little diffraction pattern. Also, we conclude that, from figure 4.5 b, that we approximately get a diffraction curve MTF after correction the aberration.

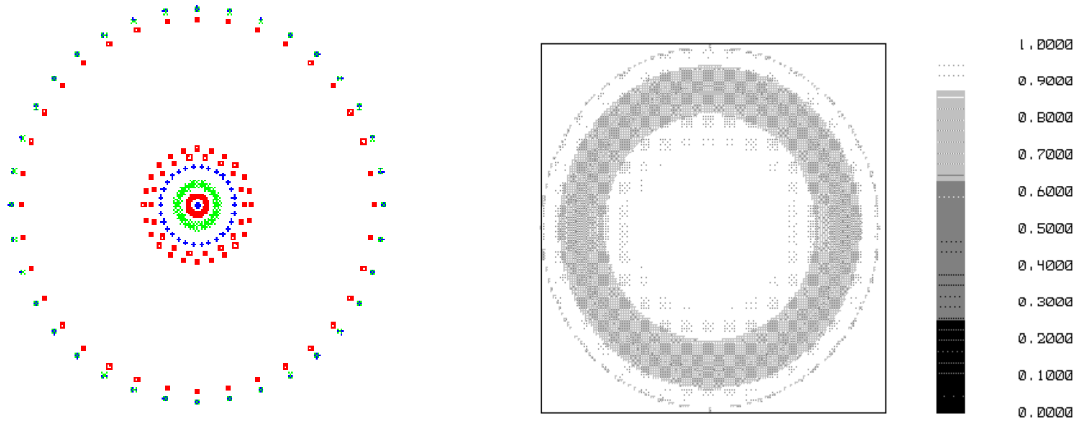

(a) spot grey pattern for **MgF_2** dome and **Sapphire** correction lens

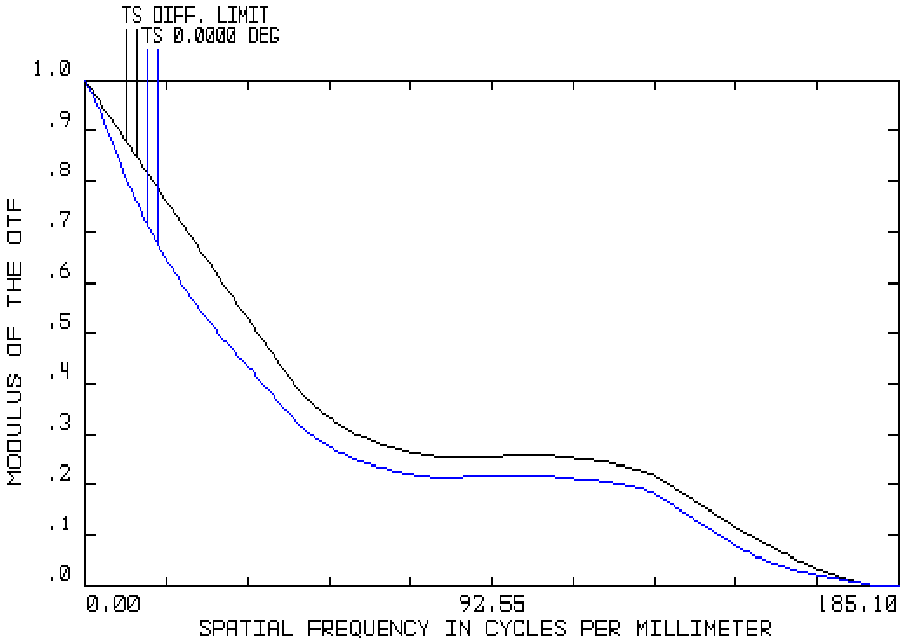

(b) Normalized MTF curve near to perfect

Figure (4.5) Result of image quality after correct the aberrations

Table (4.4) shows the result, of radius of curvature of correcting lens R_5, R_6, spot size radius, and Seidel spherical aberration "Si". These results when the dome material is sapphire.

Table 4.4 Spot size, Seidel spherical aberration, and the corresponding optimized radius of curvature (R_5) and (R_6) for **Sapphire** dome's material.

Materials of correction lens	**R_3 (mm)**	**R_4 (mm)**	**Spot size Radius (µm)**	**Si**
Germanium (n=4.025)	-33.9	-28	165.03	0.00589
Sapphire (n=1.667)	-65	-21.8	40.363	0.00493
NaCl (n= 1.5217)	Infinity	-23	147.119	0.00738
BaF2 (n=1.455)	37.5	-28	110.287	0.02226
CaF2 (n=1.41)	26	-27.95	77.109	0.0247
MgF2 (n=1.349)	26.75	-23	58.706	0.01988
LiF (n= 1.3494)	21	-25	25.047	0.02075

Table (4.4) shows that the Sapphire correction lens, which is convexo-concave lens, give aberration results, i.e. gives minimum values of Seidel aberration and small radius of spot size. After changing R_5 and R_6 we get that the spot radius is 40.363µm with such small Seidel spherical aberration equal to 0.00493.

Figure (4.6) shows the result of image quality after correcting the aberration. From Figure 4.6.a we conclude that we get better spot since it have a high intensity with little diffraction pattern. Also, we get conclude that, from

Figure 4.6.b, that we approximately get a diffraction curve MTF after correction the aberration.

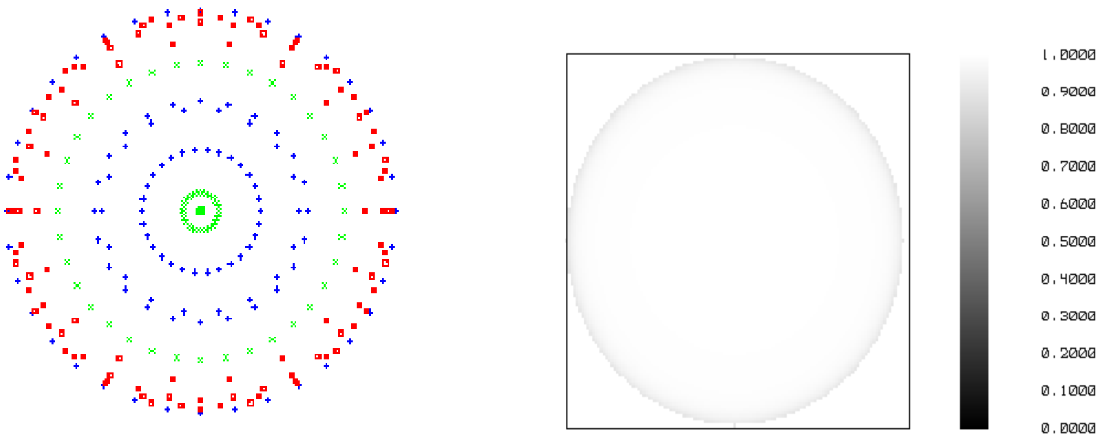

(a) spot grey pattern for the **Sapphire** dome and correction lens

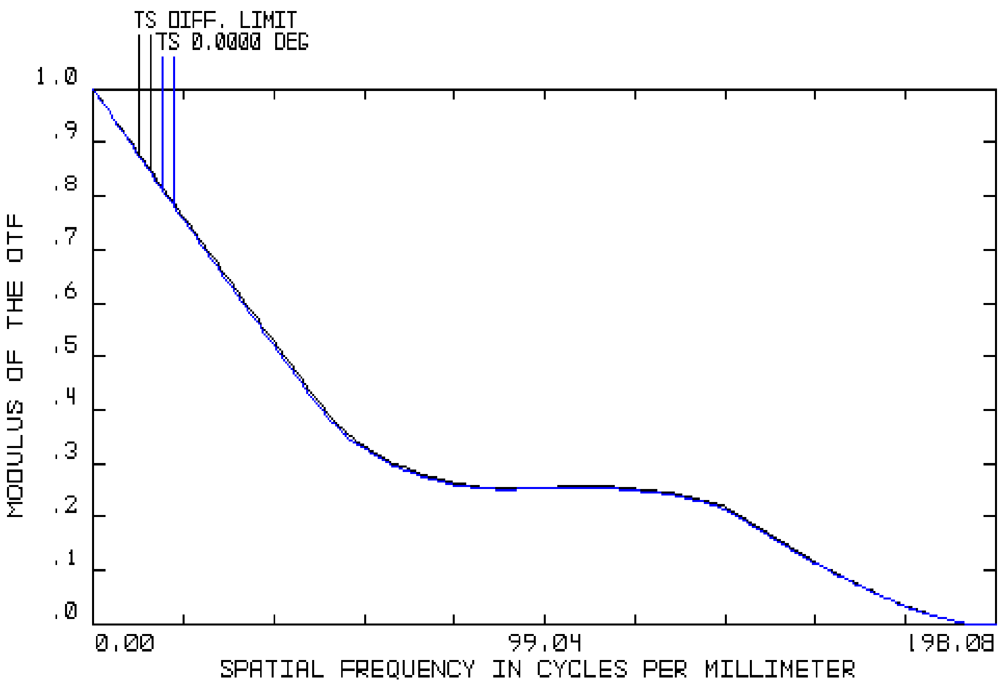

(b) Normalized MTF curve is a perfect

Figure 4.6 Result of image quality after correct the aberrations

Table (4.5) shows the result, of radius of curvature of correcting lens R_5, R_6, spot size radius, and Seidel spherical aberration "Si". These results when the dome material is LiF.

Table 4.5 Spot size, Seidel spherical aberration, and the corresponding optimized radius of curvature (R_5) and (R_6) for **LiF** dome's material.

Materials of correction lens	**R_3 (mm)**	**R_4 (mm)**	**Spot size Radius (µm)**	**Si**
Germanium (n = 4.025)	-32.2	-28	106.815	0.03818
Sapphire (n = 1.667)	-115	-28	69.406	0.03956
NaCl (n = 1.5217)	Infinity	-27.8	115.37	0.04089
BaF_2 (n = 1.455)	145	-28	108.997	0.04317
CaF_2 (n = 1.41)	78	-28	101.108	0.04322
MgF_2 (n=1.349)	41	-28	89.496	0.04423
LiF (n = 1.3494)	41	-28	71.655	0.04446

Table (4.5) shows that the Sapphire correction lens, which is convexo-concave lens, give a better results, i.e. gives minimum values of Seidel aberration and small radius of spot size. After changing R_5 and R_6 we get that the spot radius is 69.406 µm, with such small Seidel spherical aberration 0.03956.

Figure (4.7) shows the result of image quality after correcting the aberration. From Figure 4.7.a we conclude that we get better spot since it have a high intensity with little diffraction pattern. Also, we get conclude that, from

Figure 4.7.b, that we approximately get a diffraction curve MTF after correction the aberration.

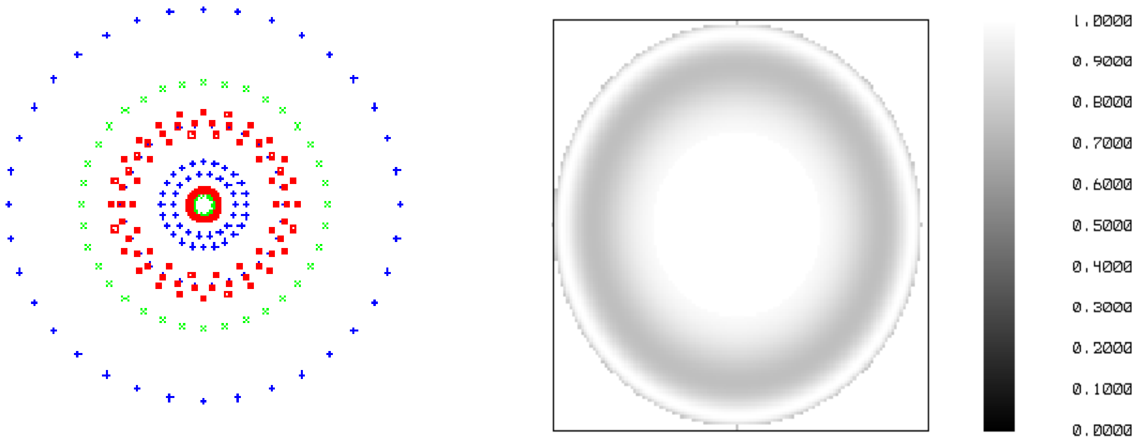

(a) spot grey pattern for the **LiF** dome and **Sapphire** correction lens

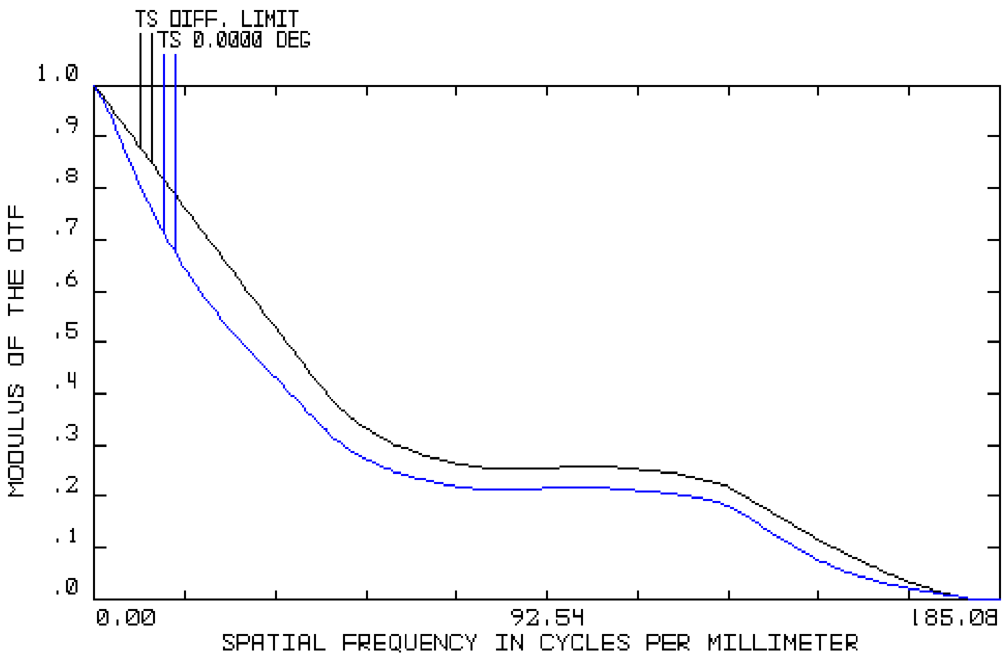

(b) Normalized MTF curve near to perfect

Figure 4.7 Result of image quality after correct the aberrations

Table (4.6) shows the result, of radius of curvature of correcting lens R_5, R_6, spot size radius, and Seidel spherical aberration ”Si”. These results when the dome material is BaF_2.

Table 4.6 Spot size, Seidel spherical aberration and the corresponding optimized radius of curvature R_5 and R_6 for **BaF_2** dome's material.

Materials of correction lens	**R_3 (mm)**	**R_4 (mm)**	**Spot size Radius (µm)**	**Si**
Germanium (n=4.025)	-33.25	-28	34.789	0.02816
Sapphire (n=1.667)	-112	-25	98.805	0.03368
NaCl (n= 1.5217)	110	-28	46.36	0.03619
BaF2 (n=1.455)	55.8	-28.05	39.164	0.03822
CaF2 (n=1.41)	37	-28	54.238	0.04
MgF2 (n=1.349)	22.35	-28	84.252	0.04085
LiF (n= 1.3494)	22.3	-28	118.611	0.04145

Table (4.6) shows that the Germanium correction lens, which is a convexo-concave lens, give a better results, i.e. gives minimum values of Seidel spherical aberration and radius of spot size. After changing R_5 and R_6 we get that the spot radius is 34.789µm ,with such small spherical aberration equal to 0.02816.

Figure (4.8) shows the result of image quality after correcting the aberration. From Figure 4.8.a we conclude that we get better spot since it have a high intensity with little diffraction pattern. Also, we get conclude that, from Figure 4.8.b, that we approximately get a diffraction curve MTF after correction the aberration.

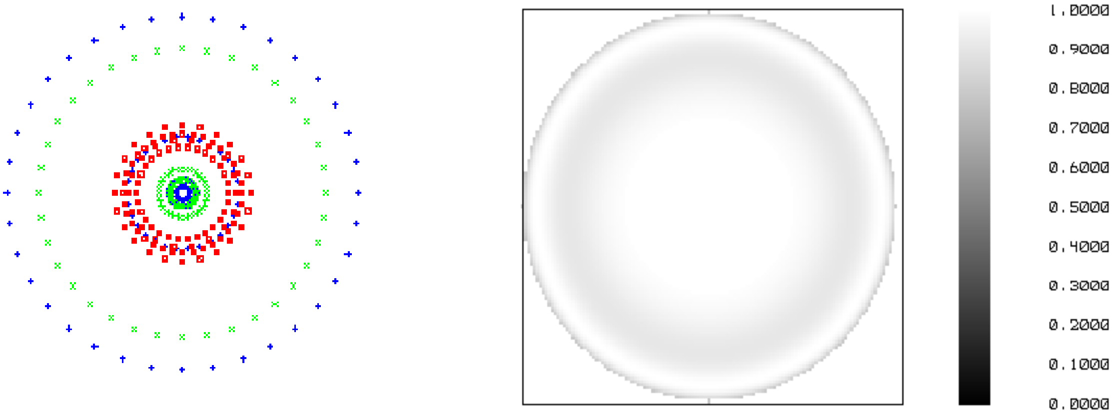

(a) spot grey pattern for the **BaF_2** dome and **Ge** correction lens

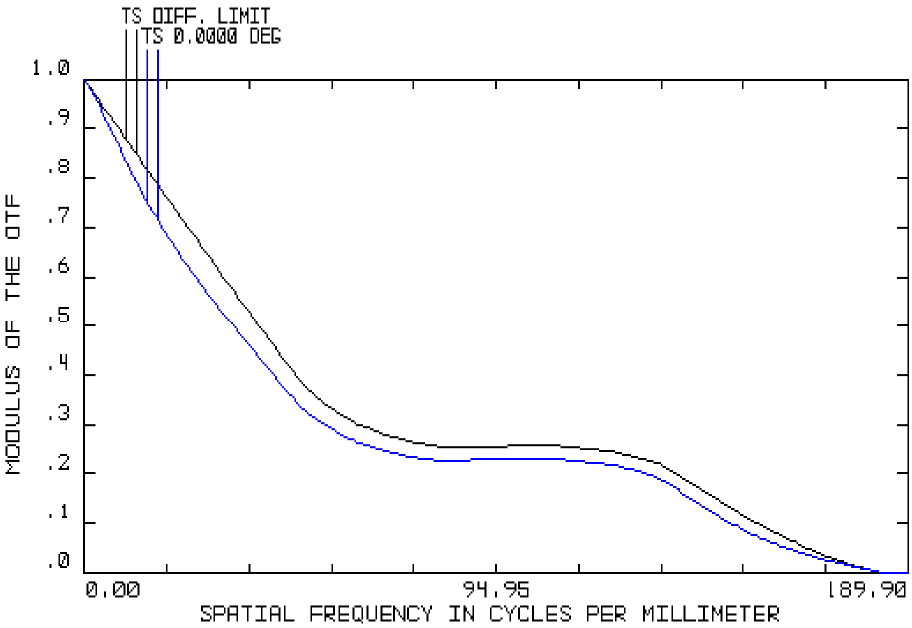

(b) MTF curve near to perfect

Figure 4.8 Result of image quality after correct the aberrations

Table (4.7) shows the result, of radius of curvature of correcting lens R_5, R_6, spot size radius, and Seidel spherical aberration "Si". These results when the dome material is CaF_2.

Table 4.7 Spot size, Seidel spherical aberration, and the corresponding optimized radius of curvature R_5 and R_6 for **CaF_2** dome's material.

Materials of correction lens	**R_3 (mm)**	**R_4 (mm)**	**Spot size Radius (µm)**	**Si**
Germanium (n = 4.025)	-33	-28	49.692	0.03645
Sapphire (n = 1.667)	-71.157393	-23.8	69.621	0.03205
NaCl (n = 1.5217)	155	-28	62.963	0.04106
BaF2 (n =1.455)	71.5	-28	59.298	0.04144
CaF2 (n=1.41)	46.6	-28	49.126	0.04126
MgF2 (n =)	27	-28	56.115	0.04299
LiF (n = 1.3494)	27	-28	84.832	0.04331

Table (4.7) shows that the Germanium correction lens, which is convexo-concave lens, give a better results, i.e. gives minimum values of Seidel aberration and small radius of spot size. After changing R_5 and R_6 we get that the spot size is 49.692µm, with such small Seidel spherical aberration equal to 0.03645.

Figure (4.9) shows the result of image quality after correcting the aberration. From Figure 4.9.a we conclude that we get better spot since it have a high intensity with little diffraction pattern. Also, we get conclude that, from Figure 4.9.b, that we approximately get a diffraction curve MTF after correction the aberration.

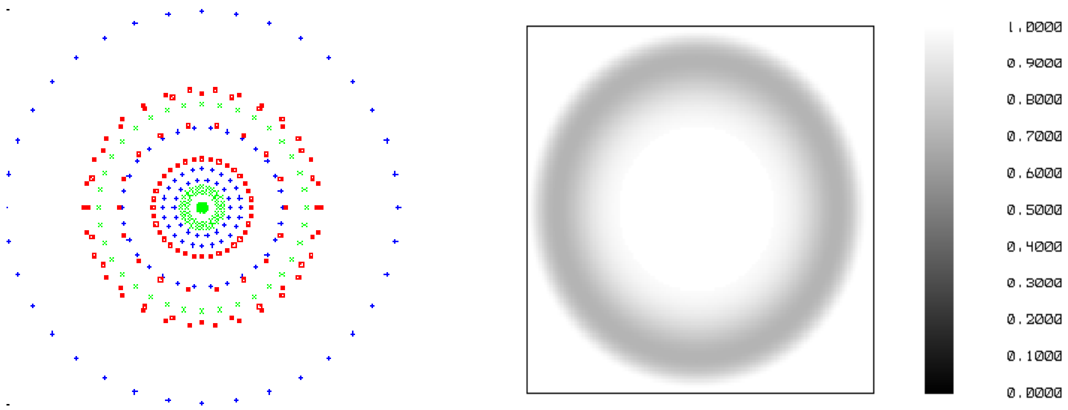

(a) spot grey pattern for the **CaF_2** dome and **Ge** correction lens

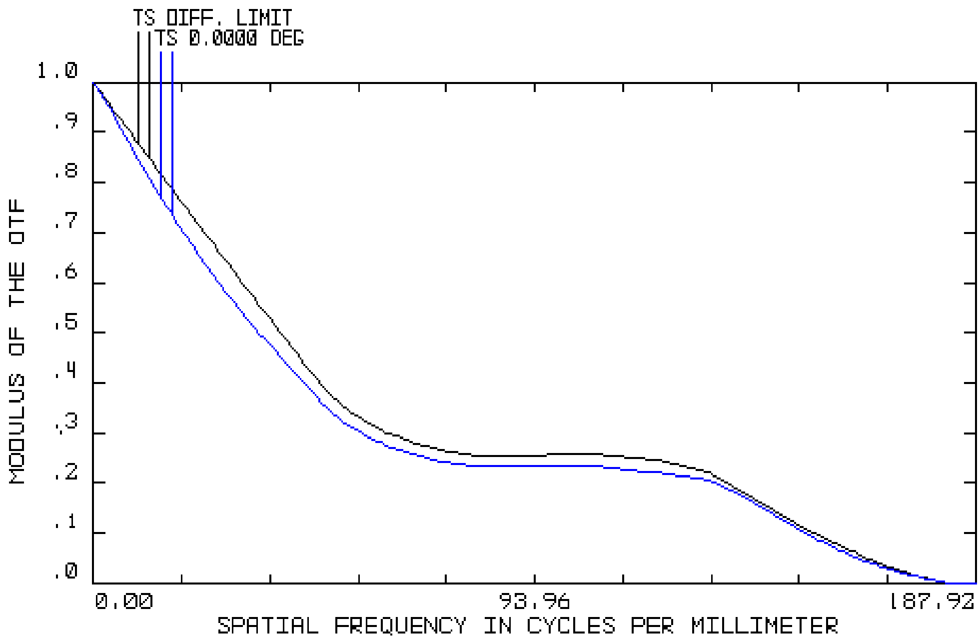

(b) Normalized MTF curve near to perfect

Figure 4.9 Result of image quality after correct the aberrations

Table (4.8) shows the result, of radius of curvature of correcting lens R_5, R_6, spot size radius, and Seidel spherical aberration "Si". These results when the dome material is NaCl.

Table 4.8 Spot size, Seidel spherical aberration and the corresponding optimized radius of curvature (R_5) and (R_6) for **NaCl** dome's material.

Materials of correction lens	**R_3 (mm)**	**R_4 (mm)**	**Spot size Radius (µm)**	**Si**
Germanium (n=4.025)	-33.65	-28	14.416	0.02404
Sapphire (n=1.667)	Infinity	-28.2	130.76	0.03414
NaCl (n= 1.5217)	80	-28	27.13	0.03377
BaF_2 (n=1.455)	45.8	-28.05	43.277	0.03357
CaF_2 (n=1.41)	31	-28	67.179	0.03608
MgF_2 (n=)	19	-28	103.362	0.03607
LiF (n= 1.3494)	19	-28	144.823	0.03696

Table (4.8) shows that the Germanium correction lens, which is convexo-concave lens, give a better results, i.e. gives minimum values of Seidel aberration and small radius of spot size. After changing R_5 and R_6we get that the spot radius is 14.416µm, with such small Seidel spherical aberration equal to 0.02404.

Figure (4.10) shows the result of image quality after correcting the aberration. From Figure 4.10.a we conclude that we get better spot since it have a high intensity with little diffraction pattern. Also, we get conclude that, from

Figure 4.10.b, that we approximately get a diffraction curve MTF after correction the aberration.

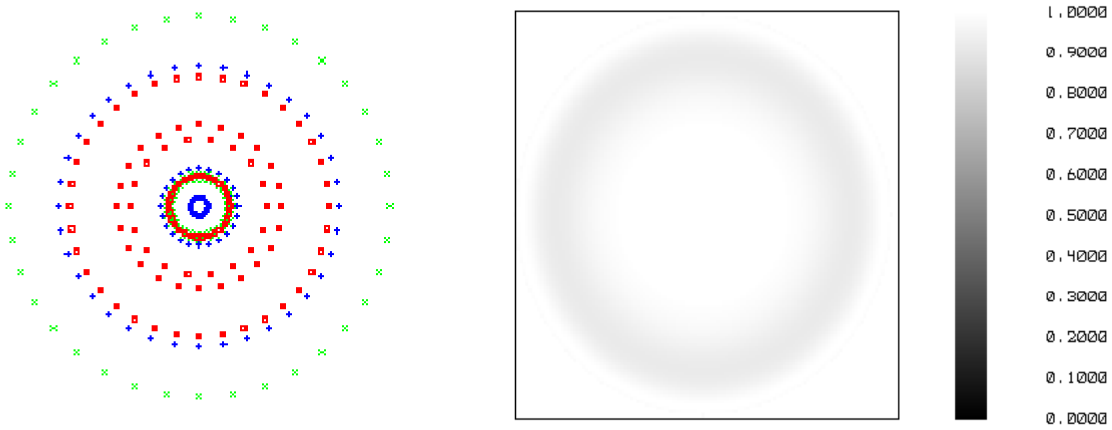

(a) spot grey pattern for the **NaCl** dome and **Ge** correction lens

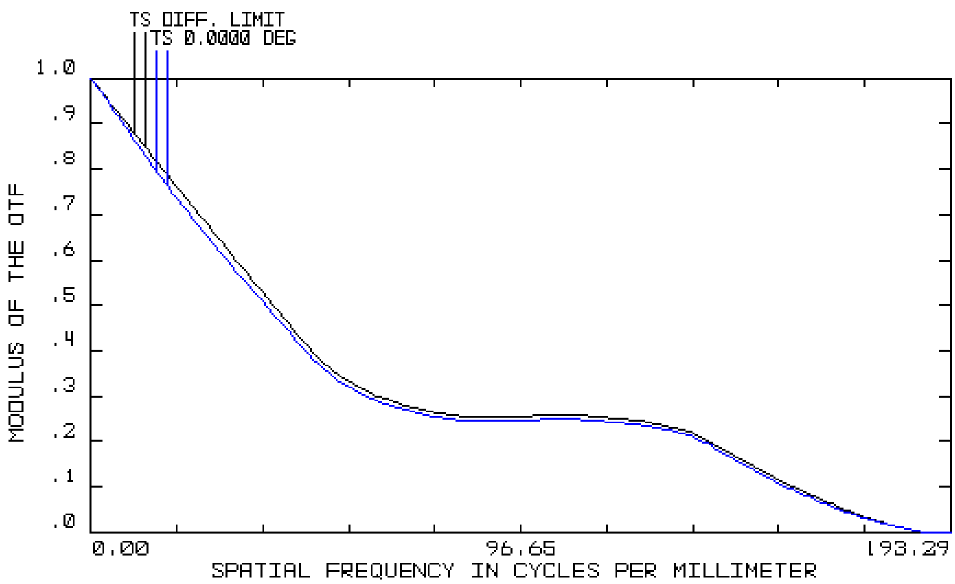

(b) Normalized MTF curve is a perfect

Figure 4.10 Result of image quality after correct the aberrations

All the above results are repeated using Germanium material for dome, this lead to change the size and the shape of the optical system.

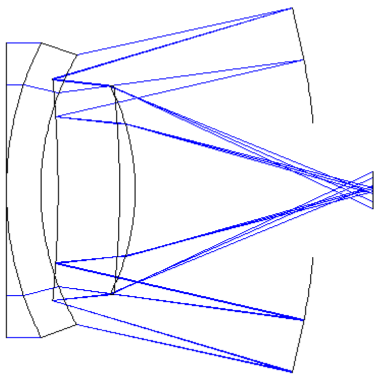

(a) Optical system design of IR homing head for **Ge** dome and **Sapphire** correction lens

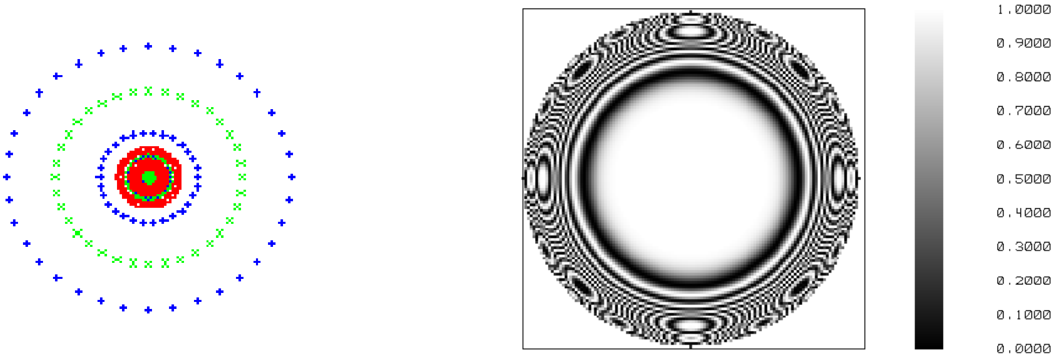

(b) spot gry pattern for the **Ge** dome and **Sapphire** correction

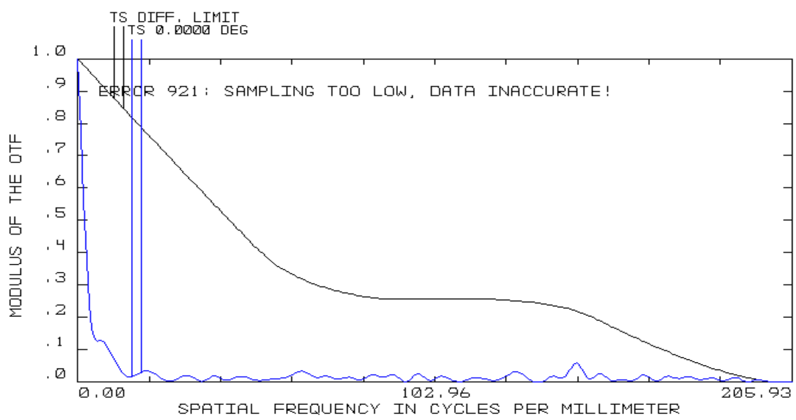

(c) Normalized MTF curve

Figure 4.11 Result of design and image when using Germanium material for dome

From Figure (4.11) we conclude that when using Germanium material for dome we get not good results. This is because of high refractive index of Germanium, which lead to highly refracted beam.

Table (4.9) shows the best final results corresponding to the dome material and correcting lens material.

Table 4.9 Final results for Domes materials, Correction lens materials, Spot size radius and Seidel spherical aberration

Dome materials	**Correction lens materials**	**Spot size radius (µm)**	**Si**
Sapphire (n=1.667)	Sapphire	40.363	0.00493
NaCl (n= 1.5217)	Germanium	14.416	0.02402
BaF_2 (n=1.455)	Germanium	34.789	0.02816
CaF_2 (n=1.41)	Germanium	49.692	0.03645
MgF_2 (n= 1.349)	Sapphire	43.143	0.03986
LiF (n= 1.3494)	Sapphire	69.406	0.03956

ABBREVIATIONS

Symbol		Unit
A	Refraction invariant	
B	Shape or bending constant	
c	Velocity of light ≈ $3*10^8$	m/s
C	Conjugate or magnification constant	
c	Curvature of refracting surface	cm^{-1}
d	diameter of the central maximum	mm
D	Diameter of the aperture	mm
E	Seidel eccentricity	
e	Optical efficiency	
F#	F-number	
f	Effective focal length	mm
h	Paraxial incidence height	mm
H	Lagrange invariant	
IR	Infrared radiation	
i	Paraxial angle of incident	

P	Lens power	diopter
MTF	Modulation Transfer Function	
n	Refractive index	
n_d	Refractive index at sodium *D*-line	
n_f	Refractive index at hydrogen *F*-line	
n_c	Refractive index at hydrogen *C*-line	
p_1, p_2	Points on lens surface	
R	Radius of curvature	mm
S_I	Seidel spherical aberration	
S_{II}	Seidel coma aberration	
S_{III}	Seidel astigmatism aberration	
S_{IV}	Seidel curvature of field aberration	
S_V	Seidel distortion aberration	
t	Thickness of the lens	mm
T	Spot size aberration constant	
u	Paraxial convergence angle	rad

v	Velocity of light in the material	m/s
V	Abbe number	
λ	Wavelength	µm
η'/η	Transverse magnification	
δ_d	Spot size	µm
θ_i	Angle of incident	degree
ϕ	Angle that the radius R_1 of the lens surface makes at the center of curvature	

References

Al-Ani A.A. [1995]
Restoration of Atmospherically Degraded Images
Ph.D. Thesis, Department of physics, College of Science, University of Baghdad, Iraq.

Al-Bakir Z. T. [2005]
Design Analysis for the Optical Elements of Solid State Laser Range Finder
M.Sc. Thesis, College of Engineering, Al-Nahrain University, Baghdad, Iraq.

Aberrations and Distortion [2005]
Via Internet: http://nikon.topica.ne.jp/bi-e/encyclo/ad.htm

Al-Kaysi S. A. [2006]
Design and Analysis of the Four Elements Objective Lens for the 3.2-4.2 µm Spectral Region
M.Sc. Thesis, Department of physics, College of Science, Al-Nahrain University, Baghdad, Iraq.

Al-Awsi S. M. [2006]
Optical System Design Improvement for IR Homing Head
Ph.D. Thesis, Department of physics, College of Science, Al-Nahrain University, Iraq.

Baker K. [1983]
Design Requirements for a Passive Infrared Homing Head
Advance Infrared Detectors and System, pp 24-26

Boutellier R. [1985]
Infrared Objective System Lens
U.S. Patent **# 4537464**

Davidson M. W [2006]
Transfer Function
The Florida State University, **32310**

Ditton R. [1998]
Modern Geometrical Optics
John Wiley: New York

Donald C. O'Shea, [1985]
Elements of Modern Optical Design
John Wiley and Sons: Atlanta

Dubner H. [1959]
Optical Design for Infrared Missile Seeker
Proceeding of the IRE, June 30 1959, pp 1537-1539

Froelich A. J. [1980]
A low-cost Infrared Seeker (LCIRS) for terminal homing
SPIE, V. 256 Infrared System, pp 37-45

Hecht E. [1998]
Optics
3rd Addison Wesley: New York

Hudson R. D. [1969]
Infrared System Engineering
John Wiley and Sons, New York

Habana S. A. [2001]
Design and evaluation of image quality for IR scanner.
Ph.D. Thesis, College of engineering, Military College, Baghdad, Iraq.

ISP Optics [2005]
General Characteristics of the Materials
Via Internet: http://www.ispoptics.com

Jenkins F. A. and White H. E. [1976]
Fundamentals of Optics
4th ed. McGraw Hill: New York

Kingslake R. [1978]
Lens Design Fundamentals
Academic Press

Laikin M. [2001]
Lens Design
Marcel Dekker: New York

Lioyd J.M. [1975]
Thermal Imaging Systems
Plenum Press: New York

Nussbaum A. [1998]
Optical System Design
Prentice Hall: USA

Optical Materials [2005]
Via Internet: sales@redoptronics.com

Optical Materials Selection Guide
Via Internet: www.janostech.com

Physics [1998]
Introduction to the Aberrations of Optical Systems
Via Internet: www.physics.montana.edu/students/thiel/docs/Aberrat.pdf

Rogers P. J. [1977]
Infrared Lenses
U.S. Patent **#4030805**

Sadiq A. A. [2000]
Computations of Wavefront Aberration Function
M.Sc. Thesis, College of Science, Al-Nahrain University (Formerly Saddam University), Baghdad, Iraq.

Scott R. M. [1959]
Optics for Infrared system
Proceeding of the IRE, June 30 1959, pp.1956-1960

Sharma K. D. [1992]
Some Infrared Materials for The Cooke Triplet Design for the 3-5µm Spectral Region: A comparison
APPLIDE OPTICS, Vol. 31, No. 1, 1992

Shannon R. R. [1997]
The Art and Science of Optical Design
Cambridge University Press: United Kingdom

Smith W. J. [1978]
Handbook of Optics
McGraw-Hill: USA

Thomson J. H. and Smith F. G. [1988]
Optics
2nd ed. John Wiley and Sons: Chichester

Welford W. T. [1974]
Aberration of the Symmetrical Optical Systems
Academic Press: London

Williams C. S. and Becklund O. A. [1986]
Optics: A Short Course for Engineering and Scientists
Robert E. Krieger Publishing Company: Florida

Zahed N. K. [2002]
Design and Analysis of an IR Homing Head for Optical Tracking
M.Sc. Thesis, College of Engineering, Al-Nahrain University (Formerly Saddam University), Baghdad, Iraq.

Zain Al-Abedeen F. S. [2004]
Atmospheric Effects on 3~5 μm Band Thermal Imaging
Ph.D. Thesis, College of Science, Al-Mustanesriyah University, Baghdad, Iraq.

المستخلص

في هذا البحث تم تبني برنامج حاسوبي لتصميم منظومة بصرية للتوجيه بعيد المدى تعمل ضمن منطقة الاشعة تحت الحمراء (Infrared) ضمن منطقة الطيف µm (3-5). لذلك يجب ان تكون المنظومة ذات خصائص عالية الجودة. تحدد كفاءة تصميم اي منظومة بصرية عن طريق دالة التضمين الانتقالي Modulation Transfer Function (MTF) وحجم البقعة. لقد تم تنفيذ العمل بمراحل وهي تصميم المنظومة وايجاد امثل تصميم لايجاد كفاءة المنظومة المقترحة.

ان مرحلة التصميم تعتمد اصلا على تصميم قياسي لرأس التوجيه الذي يعمل ضمن المنطقة تحت الحمراء، حيث تم ادخال بعض التحويرات والتحسينات على هذا التصميم للحصول على تصميم جديد بخصائص عالية الجودة. وقد شملت التحويرات اختيار المواد البصرية الملائمة لكل عنصر في المنظومة البصرية المقترحة. واختيار الصفات البصرية الملائمة لكل عنصر.

ان عمليات التحسين تم تنفيذها باستخدام برنامج Zemax لحساب الخواص البصرية المهمة الزيغ الكروي و سعة البقعة.

لقد تبين من كل النتائج ان أفضل مادة يمكن اقتراحها لمنظومة رأس التوجيه الحراري هي Sapphire عندما تستخدم في صناعة dome و correcting lens . واظهرت النتائج انه لا يمكن استخدام مادة Germanium في صناعة dome بينما يمكن استخدامها في correcting lens.

Republic of IRAQ
Ministry of Higher Education and Scientific Research
Al- Nahrain University
College of Science

A COMPUTATIONAL INVESTIGATION ON THE EFFECT OF LENS MATERIAL ON THE ABERRATIONS OF AN INFRARED OPTICAL SYSTEM

A Thesis
Submitted to the College of Science of
Al-Nahrain University in Partial Fulfillment of the
Requirements for Degree of Master of Science in
Physics

by

Haala Fadhil A. Al-Baldawi

(B.Sc. Physics 2000)

Supervisor
Dr. Ayad A. Al-Ani

Shawal **1427 A.H.**
November **2006 A.D.**

جمهورية العراق
وزارة التعليم العالي والبحث العلمي
جامعة النهرين
كلية العلوم

دراسة حاسوبية عن تأثير مادة العدسة على زيوغ منظومة بصرية تحت الحمراء

رسالة
مقدمة الى كلية العلوم في جامعة النهرين وهي جزء من متطلبات نيل درجة
ماجستير علوم فيزياء

من قبل

هالة فاضل عباس البلداوي
(بكالوريوس علوم في الفيزياء ٢٠٠٠)

المشرف
د. اياد عبد العزيز العاني

شوال ١٤٢٧ هـ

تشرين الثاني ٢٠٠٦ م